

Technical Report Documentation Page

1. REPORT No.

FHWA-CA-TL-79-09

2. GOVERNMENT ACCESSION No.**3. RECIPIENT'S CATALOG No.****4. TITLE AND SUBTITLE**

Validation of the Caline2 Model Using Other Data Bases
(Type B Study)

5. REPORT DATE

May 1979

6. PERFORMING ORGANIZATION**7. AUTHOR(S)**

Paul E. Benson and Bennett T. Squires

8. PERFORMING ORGANIZATION REPORT No.

19701-657302

9. PERFORMING ORGANIZATION NAME AND ADDRESS

Office of Transportation Laboratory
California Department of Transportation
Sacramento, California 95819

10. WORK UNIT No.**11. CONTRACT OR GRANT No.**

A-8-48

12. SPONSORING AGENCY NAME AND ADDRESS

California Department of Transportation
Sacramento, California 95807

13. TYPE OF REPORT & PERIOD COVERED

Final Report Dec 1977 to Jan 1979

14. SPONSORING AGENCY CODE**15. SUPPLEMENTARY NOTES**

This study was conducted in cooperation with the U.S. Department of Transportation, Federal Highway Administration.

16. ABSTRACT

New Gaussian vertical dispersion curves for the first 100 meters downwind of a freeway are proposed. The validity of assuming a vertical Gaussian distribution of pollutants near the freeway is examined. Results are given which indicate that traffic induced turbulence dominates at the point of emission, but that daytime variations in traffic flow have a negligible effect on the initial mixing of the pollutant at the source. Residence time within the "mixing cell", as determined by ambient wind speed, controls the initial amount of mixing that occurs.

17. KEYWORDS

Line source model, dispersion curves, mixing cell, CD concentrations, Gaussian

18. No. OF PAGES:

67

19. DRI WEBSITE LINK

<http://www.dot.ca.gov/hq/research/researchreports/1978-1980/79-09.pdf>

20. FILE NAME

79-09.pdf

TECHNICAL REPORT STANDARD TITLE PAGE

1. REPORT NO. FHWA-CA-TL-79-09	2. GOVERNMENT ACCESSION NO.	3. RECIPIENT'S CATALOG NO.	
4. TITLE AND SUBTITLE VALIDATION OF THE CALINE2 MODEL USING OTHER DATA BASES (TYPE B STUDY)		5. REPORT DATE May 1979	
		6. PERFORMING ORGANIZATION CODE	
7. AUTHOR(S) Paul E. Benson and Bennett T. Squires		8. PERFORMING ORGANIZATION REPORT NO. 19701-657302	
9. PERFORMING ORGANIZATION NAME AND ADDRESS Office of Transportation Laboratory California Department of Transportation Sacramento, California 95819		10. WORK UNIT NO.	
		11. CONTRACT OR GRANT NO. A-8-48	
12. SPONSORING AGENCY NAME AND ADDRESS California Department of Transportation Sacramento, California 95807		13. TYPE OF REPORT & PERIOD COVERED Final Report Dec 1977 to Jan 1979	
		14. SPONSORING AGENCY CODE	
15. SUPPLEMENTARY NOTES This study was conducted in cooperation with the U.S. Department of Transportation, Federal Highway Administration.			
16. ABSTRACT New Gaussian vertical dispersion curves for the first 100 meters downwind of a freeway are proposed. The validity of assuming a vertical Gaussian distribution of pollutants near the freeway is examined. Results are given which indicate that traffic induced turbulence dominates at the point of emission, but that daytime variations in traffic flow have a negligible effect on the initial mixing of the pollutant at the source. Residence time within the "mixing cell", as determined by ambient wind speed, controls the initial amount of mixing that occurs.			
17. KEY WORDS Line source model, dispersion curves, mixing cell, CO concentrations, Gaussian.		18. DISTRIBUTION STATEMENT No restrictions. This document is available to the public through the National Technical Information Service, Springfield, VA 22161.	
19. SECURITY CLASSIF. (OF THIS REPORT) Unclassified	20. SECURITY CLASSIF. (OF THIS PAGE) Unclassified	21. NO. OF PAGES 67	22. PRICE

DS-TL-1242 (Rev.6/76)

STATE OF CALIFORNIA
DEPARTMENT OF TRANSPORTATION
DIVISION OF CONSTRUCTION
OFFICE OF TRANSPORTATION LABORATORY

May 1979

FHWA No. A-8-48
TL No. 657302

Mr. C. E. Forbes
Chief Engineer

Dear Sir:

I have approved and now submit for your information this
final research project report titled:

VALIDATION OF THE CALINE2 MODEL USING
OTHER DATA BASES (TYPE B STUDY)

Study made by Enviro-Chemical Branch
Under the Supervision of Earl C. Shirley
Principal Investigators Roy W. Bushey and
Paul E. Benson
Co-Investigator Bennett T. Squires
Report Prepared by Paul E. Benson and
Bennett T. Squires

Very truly yours,



NEAL ANDERSEN
Chief, Office of Transportation Laboratory

Attachment

BTS:1b

ACKNOWLEDGEMENTS

This report has been authored by Paul E. Benson, with the assistance of Bennett T. Squires, under the supervision of Roy W. Bushey. Ronald D. Duncan helped with the computer input, Tables, and Figures for the report. Gurlabh S. Vidwan performed some preliminary analysis of the Los Angeles Catalyst Study Data Base.

This study was conducted under Research Item A-8-48 (1-D-28) from the Federal Highway Administration titled "Validation of the CALINE2 Model Using Other Data Bases (Type B Study)".

CONVERSION FACTORS

English to Metric System (SI) of Measurement

<u>Quantity</u>	<u>English unit</u>	<u>Multiply by</u>	<u>To get metric equivalent</u>
Length	inches (in) or (")	25.40 .02540	millimetres (mm) metres (m)
	feet (ft) or (')	.3048	metres (m)
	miles (mi)	1.609	kilometres (km)
Area	square inches (in ²)	6.432 x 10 ⁻⁴	square metres (m ²)
	square feet (ft ²)	.09290	square metres (m ²)
	acres	.4047	hectares (ha)
Volume	gallons (gal)	3.785	litres (l)
	cubic feet (ft ³)	.02832	cubic metres (m ³)
	cubic yards (yd ³)	.7646	cubic metres (m ³)
Volume/Time (Flow)	cubic feet per second (ft ³ /s)	28.317	litres per second (l/s)
	gallons per minute (gal/min)	.06309	litres per second (l/s)
Mass	pounds (lb)	.4536	kilograms (kg)
Velocity	miles per hour (mph)	.4470	metres per second (m/s)
	feet per second (fps)	.3048	metres per second (m/s)
Acceleration	feet per second squared (ft/s ²)	.3048	metres per second squared (m/s ²)
	acceleration due to force of gravity (G)	9.807	metres per second squared (m/s ²)
Weight Density	pounds per cubic (lb/ft ³)	16.02	kilograms per cubic metre (kg/m ³)
Force	pounds (lbs)	4.448	newtons (N)
	kips (1000 lbs)	4.448	newtons (N)
Thermal Energy	British thermal unit (BTU)	1055	joules (J)
Mechanical Energy	foot-pounds (ft-lb)	1.356	joules (J)
	foot-kips (ft-k)	1.356	joules (J)
Bending Moment or Torque	inch-pounds (ft-lbs)	.1130	newton-metres (Nm)
	foot-pounds (ft-lbs)	1.356	newton-metres (Nm)
Pressure	pounds per square inch (psi)	6895	pascals (Pa)
	pounds per square foot (psf)	47.88	pascals (Pa)
Stress Intensity	kips per square inch square root inch (ksi \sqrt{in})	1.0988	mega pascals $\sqrt{\text{metre}}$ (MPa \sqrt{m})
	pounds per square inch square root inch (psi \sqrt{in})	1.0988	kilo pascals $\sqrt{\text{metre}}$ (KPa \sqrt{m})
Plane Angle	degrees (°)	0.0175	radians (rad)
Temperature	degrees fahrenheit (F)	$\frac{t_F - 32}{1.8} = t_C$	degrees celsius (°C)

TABLE OF CONTENTS

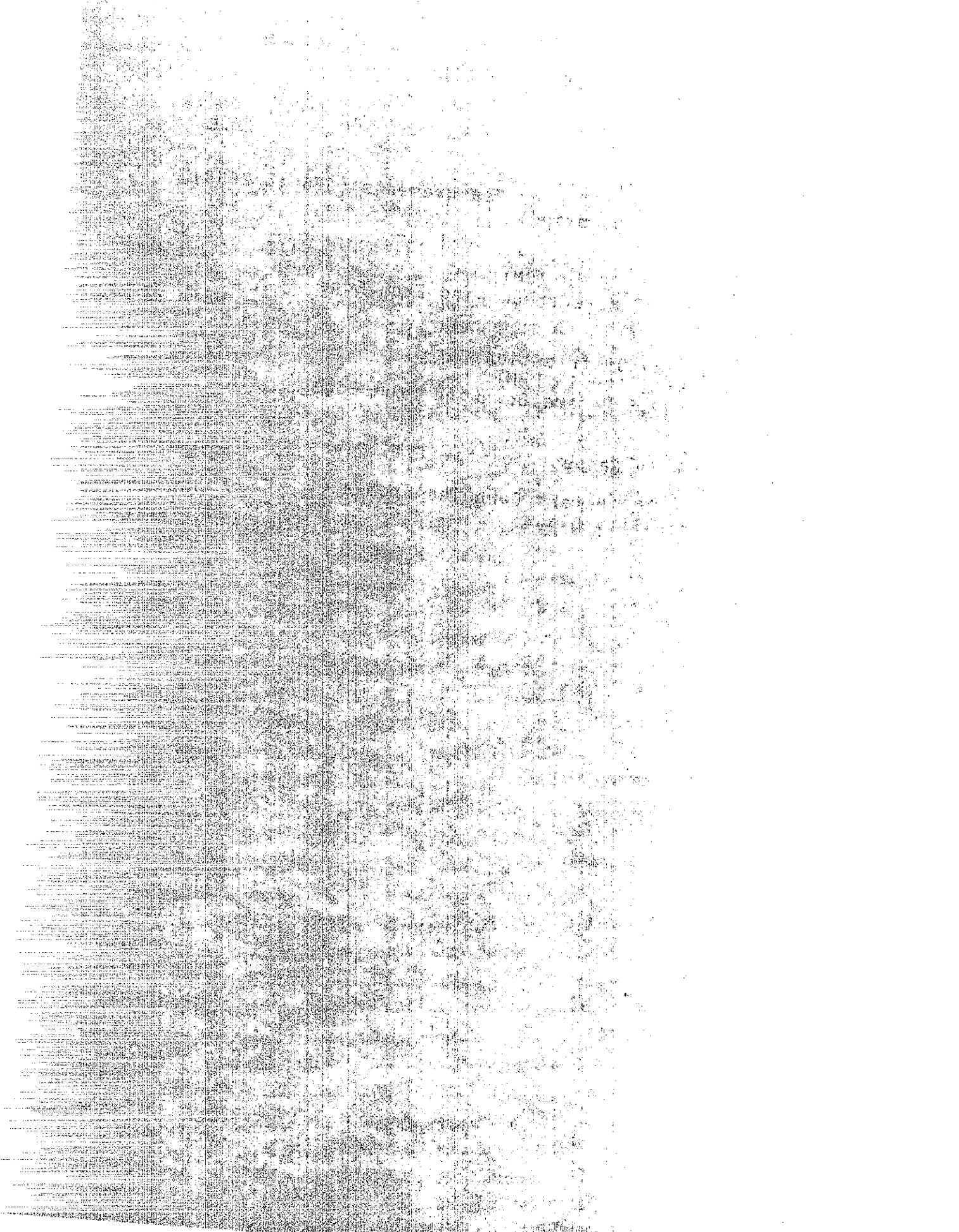
	<u>Page</u>
INTRODUCTION AND BACKGROUND	1
CONCLUSIONS AND RECOMMENDATIONS	5
IMPLEMENTATION	6
DESCRIPTION OF DATA BASES	7
DETERMINATION OF σ_z CURVES NEAR THE FREEWAY	11

LIST OF TABLES

<u>Table No.</u>		<u>Page</u>
1	Vertical Dispersion Parameter (Sigma Z) Calculated From Ground Level SF6 Concentrations General Motors Sulfate Experiment Data	14
2	Vertical Dispersion Parameter (Sigma Z) Calculated From Ground Level CO Concentrations Stanford Research Institute At-Grade Site Data	15
3	Vertical Dispersion Parameter (Sigma Z) Calculated From Ground Level SF6 Concentrations New York "Road" Project Data	16
4	Best Fit Gaussian Distribution GM Sulfate Experiment Tracer Measurements (SF6 in PPHB) Tower 4 (2 Meters Downwind)	17
5	Best Fit Gaussian Distribution GM Sulfate Experiment Tracer Measurements (SF6 in PPHB) Tower 5 (15 Meters Downwind)	18
6	Best Fit Gaussian Distribution GM Sulfate Experiment Tracer Measurements (SF6 in PPHB) Tower 6 (30 Meters Downwind)	19
7	Best Fit Gaussian Distribution SRI At-Grade Site (CO in PPM) Tower 2 or 4 (10.7 Meters Downwind From Edge of Roadway)	20
8	Best Fit Gaussian Distribution SRI At-Grade Site (CO in PPM) Tower 1 or 5 (30.5 Meters Downwind From Edge of Roadway)	21
9	Best Fit Gaussian Distribution New York Data (SF6 in PPHB) Tower 5 or 9 (4 Meters Downwind From Edge of Roadway)	22
10	Best Fit Gaussian Distribution GM Sulfate Experiment Tracer Measurements (SF6 in PPHB) Tower 4 (2 Meters Downwind)	27
11	Best Fit Gaussian Distribution GM Sulfate Experiment Tracer Measurements (SF6 in PPHB) Tower 5 (15 Meters Downwind)	28

LIST OF TABLES (con't.)

<u>Table No.</u>		<u>Page</u>
12	Best Fit Gaussian Distribution GM Sulfate Experiment Tracer Measurements (SF6 in PPHB) Tower 6 (30 Meters Downwind)	29
13	Best Fit Gaussian Distribution SRI At-Grade Site (CO in PPM) Tower 2 or 4 (10.7 Meters Downwind From Edge of Roadway)	30
14	Best Fit Gaussian Distribution SRI At-Grade Site (CO in PPM) Tower 1 or 5 (30.5 Meters Downwind From Edge of Roadway)	31
15	r^2 , α , and β With Respect to Stability Class	38
16	α and β Within 100 Meters Downwind From a Freeway by Stability Class	54



LIST OF FIGURES

<u>Figure No.</u>		<u>Page</u>
1	Vertical Dispersion Parameters Used in Caline 2 Program	2
2	Various vertical dispersion parameter plots perpendicular to a highway VS. distance from the highway.	4
3	Probe Locations (Site 1) Santa Monica Fwy. at 4th Ave. Pedestrian Overcrossing	8
4	Meteorological Instrumentation (Site 1) Santa Monica Fwy. at 4th Ave. Pedestrian Overcrossing	9
5	Probe Locations, Site 3, San Diego Fwy. at 134th Street	10
6	Average Measured and Residual SF ₆ Concentrations	23
7	Average Measured and Residual CO Concentrations	24
8	Average Measured and Predicted SF ₆ Concentrations	33
9	σ_z as Calculated from Observed Concentrations Under "B" Stability	34
10	σ_z as Calculated from Observed Concentrations Under "C" Stability	35
11	σ_z as Calculated from Observed Concentrations Under "D" Stability	36
12	σ_z as Calculated from Observed Concentrations Under "F" Stability	37
13	Temporal Patterns for January 28, 1975 (SRI At-Grade Site)	40
14	Temporal Patterns for January 30, 1975 (SRI At-Grade Site)	41
15	Temporal Patterns for February 5, 1975 (SRI At-Grade Site)	42

LIST OF FIGURES (con't.)

<u>Figure No.</u>		<u>Page</u>
16	Best Fit σ_z at 10 Meter Tower Versus Traffic Volume	44
17	Best Fit σ_z at 10 Meter Tower Versus Traffic Energy Index	45
18	Roadway Turbulence Measured at 2 Meter Height, Versus Traffic Volume	46
19	Roadway Turbulence Measured at 2 Meter Height, Versus Traffic Energy Index	47
20	Roadway Turbulence, Measured at Z = 3.8 Meters Versus Traffic Energy Index	48
21	Evaluation of Bivane Results at Z = 3.8 Meters	50
22	Best Fit σ_z Near Downwind Edge of Roadway Versus Wind Speed	52
23	Paired Upwind and Downwind Values of U at Z = 3.8 Meters	53
24	Comparison of Present CALINE-2 Curves to Three Representative Cases of Recommended Sigma Z Curve Model	55

INTRODUCTION AND BACKGROUND

Recent validation studies by Noll(1), Maldonado and Bullin(2) and Benson(3) have revealed the tendency for the Gaussian line source dispersion model, CALINE2, to underpredict CO concentrations near freeways during neutral to unstable, crosswind conditions and overpredict for stable, parallel wind conditions. This report examines vertical dispersion parameters near the highway under crosswind conditions. Further research is being conducted to correct for parallel wind overpredictions using this initial crosswind study as a basis for modeling parallel wind vertical dispersion near the highway.

The integrated form of the Gaussian expression used by CALINE2 for crosswind conditions is:

$$C(x, y, z) = \frac{q}{(2\pi)^{\frac{1}{2}} \sigma_z u} \left\{ \exp\left[\frac{-(z-H)^2}{2\sigma_z^2}\right] + \exp\left[\frac{-(z+H)^2}{2\sigma_z^2}\right] \right\}$$

where, C = concentration
 q = source strength/unit distance
 u = wind speed
 H = source height
 Z = sampling height
 σ_z = vertical dispersion parameter

Since all the terms in this equation, except σ_z are usually accurately determined in validation studies, it seems reasonable to investigate the σ_z curves used by the model in order to explain the underprediction for the crosswind case. Those curves, shown in Figure 1, were based on

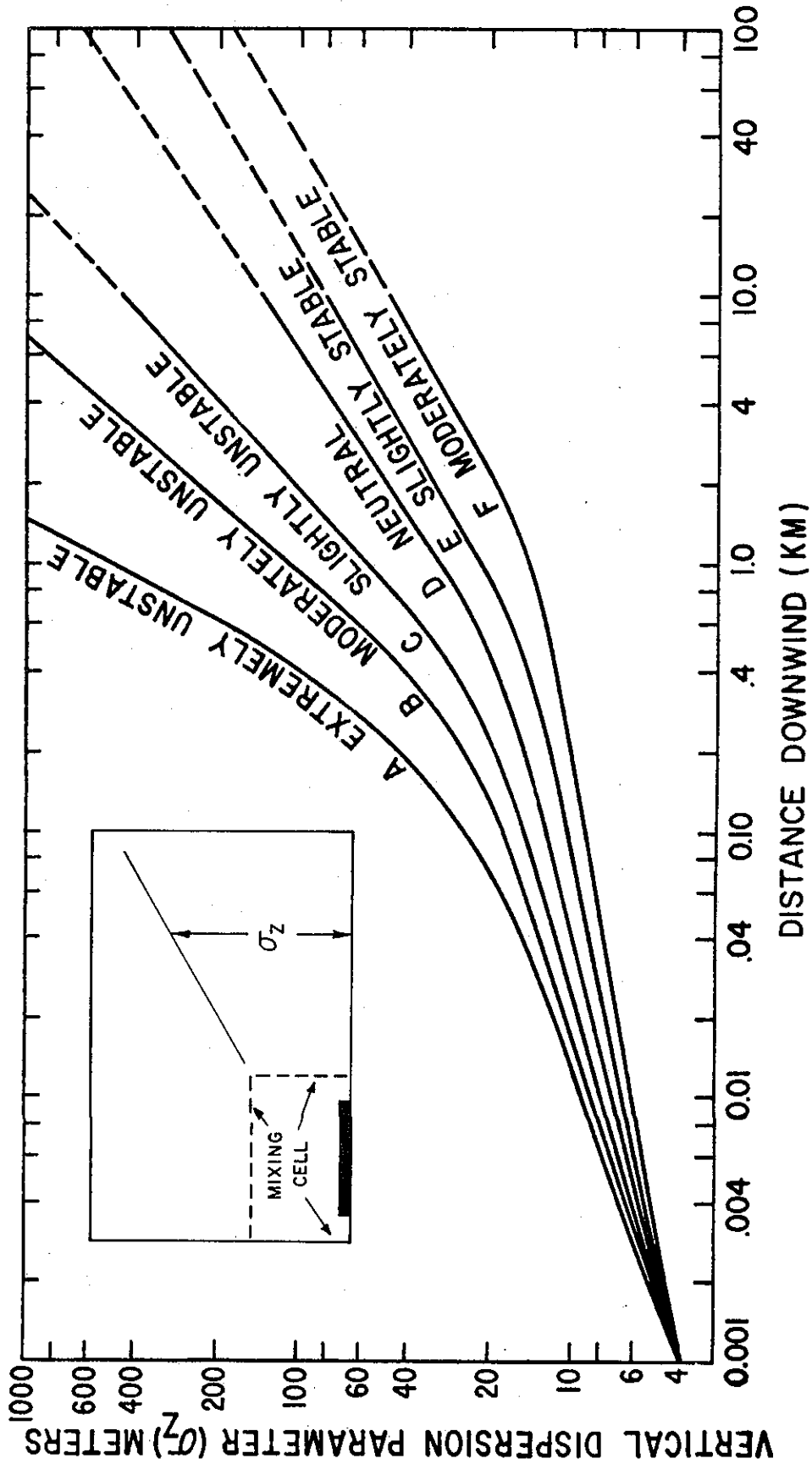


FIG. 1 VERTICAL DISPERSION PARAMETERS
USED IN CALINE 2 PROGRAM

visual observations of the vertical dispersion of a smoke tracer behind a single car (4). This paper details the results of a more comprehensive approach used to revise these curves. Analyses of existing data bases were used as the basis to reformulate the σ_z curves. No field measurements were undertaken as part of this study.

In the current literature, there are a variety of σ_z curves for the modeler to choose from. Hanna, et al (5), in their Summary of Recommendations make it clear that site conditions (urban versus rural or rough versus smooth terrain) and source exposure (elevated versus ground release) should be considered when choosing a set of curves. Immediately downwind of a freeway, however, the condition of horizontal homogeneity under which all these recommended curves are derived does not exist. Instead, there is a peak turbulence over the freeway gradually decaying to ambient levels some distance downwind. Johnson (6) has constructed σ_z curves for freeways based on tracer data, but his results indicate that the σ_z values used in CALINE2 are too small (see Figure 2). Since the experience to date is that CALINE2 underpredicts for the crosswind condition, use of Johnson's still greater values for σ_z would lead to even more serious under prediction by the model. Draxler (7) has suggested a method for predicting σ_z from in situ measurements of the standard deviation of the vertical wind angle σ_ϕ . Again the lack of horizontal homogeneity, plus the fact that σ_ϕ measurements "before" construction would be meaningless to predict "after" conditions, make this approach impractical for freeways.

A number of field studies concerning dispersion of pollutants near freeways have been made. Rao and Sedefian (9)

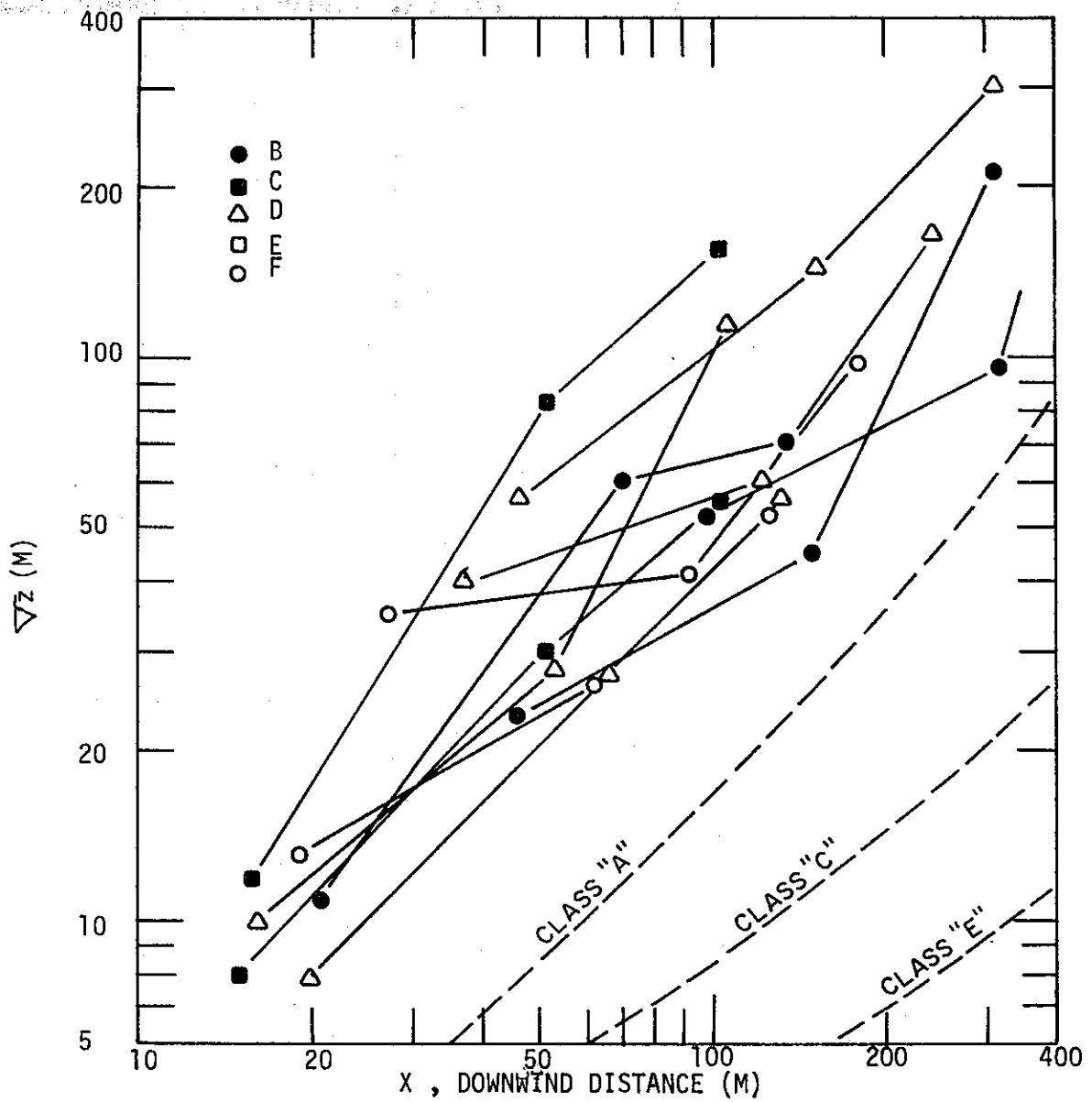


Fig. 2 Various vertical diffusion (σ_z) plots perpendicular to a highway VS. distance from the highway. Pasquill stability curves are shown for comparison.

After Johnson (1974)

have made detailed spectral analyses of turbulence near a freeway and conclude that under smooth traffic flow and neutral to unstable atmospheric conditions the mechanical turbulence added by the cars is significant, while thermal turbulence from automotive exhaust heat is not. Dabberdt(10) and Chock(11), analyzing heavier traffic flows and more stable atmospheric conditions, conclude that waste heat from the traffic does add significantly to near freeway turbulence.

In light of the problems with CALINE2 and the lack of a clear solution in the literature, it was felt that an analysis of several independent data bases might yield a set of reliable σ_z curves to be used for freeway applications.

CONCLUSIONS AND RECOMMENDATIONS

Based on Tracer (SF_6) concentrations measured during the GM Sulfate Experiment, Gaussian curves can adequately describe the vertical dispersion of relatively inert pollutants under crosswind conditions in the area between the highway (the so-called mixing cell) and 100 meters out from the highway. Initial vertical dispersion is related to wind speed or residence time within the mixing cell. At higher wind speeds initial vertical dispersion is reduced. The shortcomings of the existing CALINE2 line source model are its lack of detail in describing 1) the residence time of the polluted air within the mixing cell, and 2) the turbulence energy budget within the mixing cell.

Although this report suggests new vertical dispersion curves which include the effect of mixing cell vehicle turbulence, a current research project to thoroughly

study these two items will soon lead to more accurate estimates of both σ_y and σ_z curves near highways. This project will also include a study of currently accepted Pasquill dispersion curves to determine the feasibility of modifying them such that surface roughness effects are considered. Investigation of the adequacy of Pasquill's horizontal dispersion curve (σ_y) in the area within 100 meters of a highway line source will also be conducted.

IMPLEMENTATION

The findings of this research effort are being used to develop an improved line source model, CALINE3. It is anticipated that CALINE3 will eliminate both the under-predictions for crosswind, unstable cases and the over-predictions for parallel wind, stable conditions. The new model will also incorporate traffic and ground roughness effects on the dispersion parameters (σ_z and σ_y), and will allow for the input of the length of highway actually contributing to receptor concentrations during parallel winds. Overall, the new model will be more flexible and more accurate than its predecessor, CALINE2.

DESCRIPTION OF DATA BASES

Data used for this study were gathered from five independent field studies. The first two were carried out in Los Angeles and represented heavily urbanized sites with large traffic volumes. The three other bases involved

tracer gas controls and were conducted for at-grade freeways in relatively uncomplicated terrain. A brief description of each study follows.

Study 1

Caltrans' own data from sites on the freeway "surveillance loop" in the Los Angeles basin were used for early CALINE2 validation trials. Locations were chosen to represent various roadway configurations. The configurations included in this study were a depressed section and an elevated section. See Figures 3, 4 and 5.

Study 2

The Environmental Protection Agency's "Los Angeles Calyst Study" data were obtained and used with limited success. It is believed that a nearby city street tended to bias the relationship of the pollutant concentrations to the freeway traffic volume. The site is along the San Diego Freeway north of the Santa Monica Freeway.

Study 3

The General Motors (G.M.) Sulfate Experiment(12) represented the most controlled conditions and consequently had the least scatter in results. The experiment was conducted at the G.M. Milford, Michigan Proving Grounds Straightaway Track (5 Km long) surrounded by lightly wooded, rolling hills. Three hundred fifty-three cars (8 tracer vehicles) were driven at 80 Km/hr simulating a traffic flow of 5,462 vehicles per hour (VPH) along a 4-lane freeway.

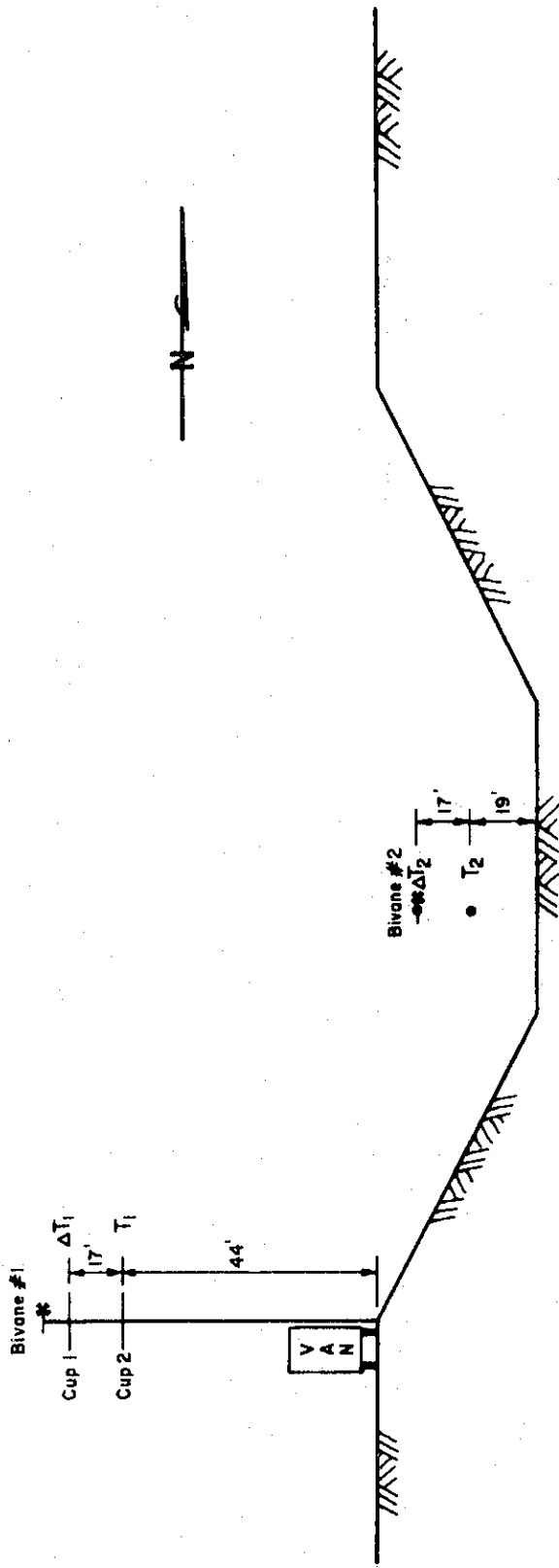
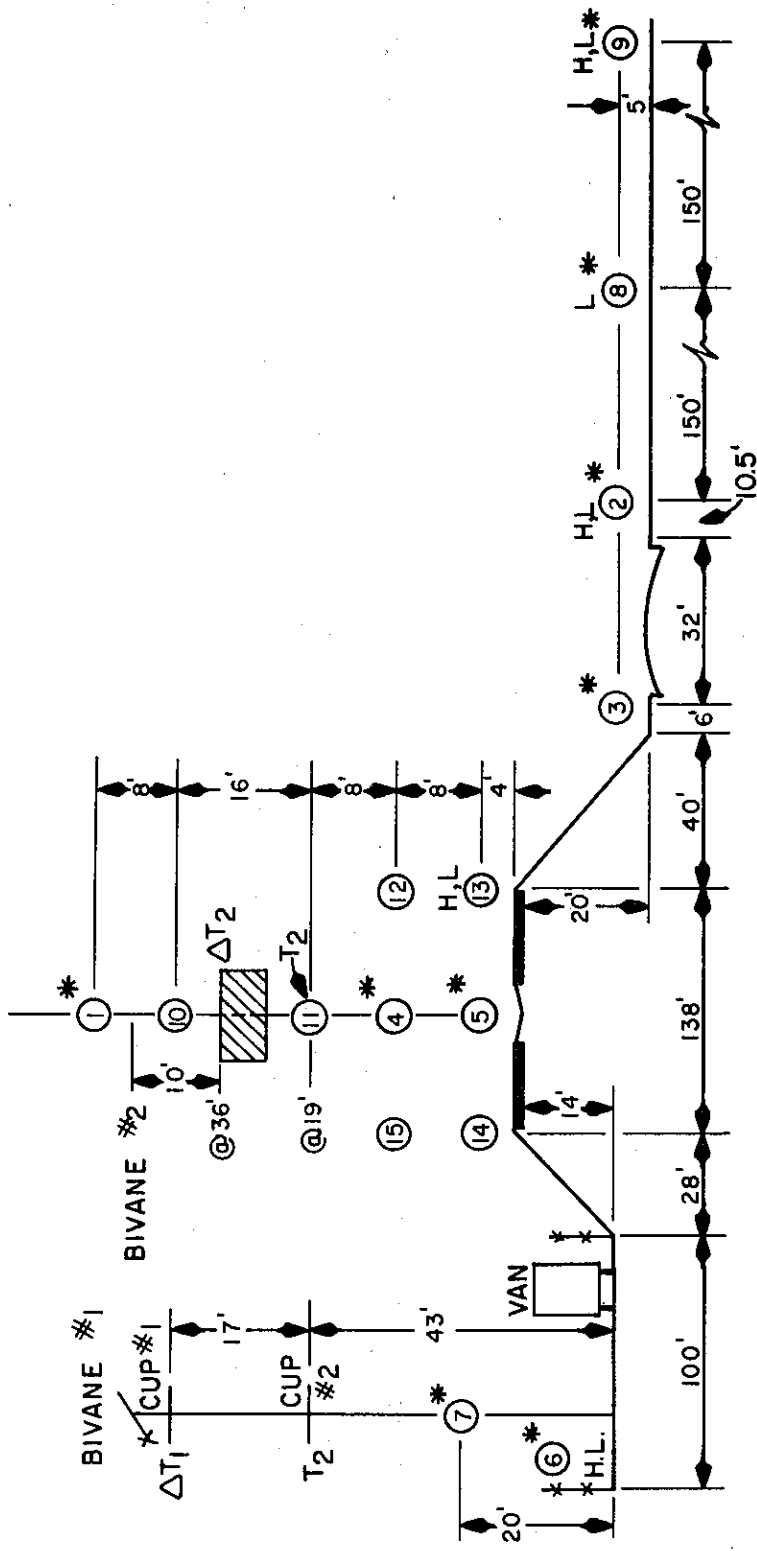


FIG. 4 METEOROLOGICAL INSTRUMENTATION (SITE I)
 SANTA MONICA FWY. AT 4TH. P.O.C.
 (1973-74)

(NOT TO SCALE)



LEGEND

- ③ = PROBE NUMBER
- * = PROBE FOR BAG BOX
- L = LUNDGREN IMPACTOR
- H = HI VOL SAMPLER

FIG. 5 PROBE LOCATIONS, SITE 3, SAN DIEGO FWY. AT 134TH STREET (1974-75)

(NOT TO SCALE)

Study 4

Another tracer study, conducted by the Stanford Research Institute (SRI) along Route 101 near San Jose, California, was in a generally urban and industrial situation. Several empty fields surrounded the multi-lane divided freeway(13). This represented more realistic freeway conditions with varying traffic flow and emissions from each vehicle (tracer results were used to deduce CO emission rates),

Study 5

A third tracer study was conducted by the New York Department of Environmental Conservation along the Long Island Expressway in New York(14), and represented medium traffic volumes in a suburban setting. Only preliminary data were available for this study.

DETERMINATION OF σ_z CURVES NEAR THE FREEWAY

For purposes of determining σ_z from measured concentrations, the data from the three tracer controlled field experiments were divided into ground level results and tower results. Tower results were obtained from vertical arrays of 3 to 4 probes. Either ground or tower results could be used to establish σ_z curves, while the tower results would also indicate how well the Gaussian model fit the observations.

Ground Level Analysis

Estimates of σ_z using the ground level data were made using

$$\sigma_z = \frac{2q}{(2\pi)^{\frac{1}{2}} u C} \exp\left[-\frac{1}{2}\left(\frac{z}{\sigma_z}\right)^2\right]$$

(terms same as Equation 1)

Wind speeds for the GM and SRI results were measured 30 M. upwind of the sites at $Z = 4.5$ M. and $Z = 3.8$ M., respectively. The only wind speeds submitted with the preliminary NY data were measured in the median at $Z = 8.0$ M. For this reason the final σ_z curves were based on only the GM and SRI results.

Tables 1 and 2 give σ_z results for the ground level analyses. The NY σ_z results, although not used in the final analysis, are included as Table 3. Note that PHI represents the horizontal angle between the wind direction and the highway (crosswind: PHI = 90°, parallel wind: PHI = 0°) and is not to be confused with the vertical wind angle (ϕ) and its standard deviation.

Tower Analysis

The following P-normal equation(16) was formulated to find the best fit σ_z to the tower data.

$$\sum_{i=1}^N \left[Y_i - \hat{Y}_i \right] \cdot \left[\left(\frac{z_i}{\hat{\sigma}_z} \right)^2 - 1 \right] \cdot \frac{\hat{Y}_i}{\hat{\sigma}_z} = 0$$

where Y_i = observed concentration

$$\hat{Y}_i = \frac{2q}{(2\pi)^{\frac{1}{2}} u \hat{\sigma}_z} \exp\left[-\frac{1}{2}\left(\frac{z}{\hat{\sigma}_z}\right)^2\right]$$

$\hat{\sigma}_z$ = best fit σ_z

N = number of vertical probes

An iterative computer program was used to solve for σ_z . The results are given as Tables 4 thru 6 for the GM data, Tables 7 and 8 for the SRI data, and Table 9 for the NY data (also not used).

An examination of the average residual differences (YHAT-Y) between predicted (YHAT) and observed (Y) results for the GM and SRI tower data was made. Figures 6 and 7 summarize the residuals and compare them to the observed concentrations. For ground level results the residuals are essentially insignificant, but significant bias is indicated by their consistent negative values. In fact, this systematic bias is shown at practically all locations. The implication is that either the source strength or wind speed are improperly characterized or that the concentrations are not normally distributed.

If wind speed were a significant problem one would expect negative residuals at low levels, zero residuals at medium heights where the wind speed was measured, and positive values at high levels. The observed residuals do not fit this pattern.

A lack of normality would also cause a systematic irregularity in the residuals as a function of height, averaging to zero at a particular tower. While this may exist as an underlying perturbation in the observed residual distributions, it does not appear to be significant. This is additionally supported by Sethu Raman and Tichler(17) who concluded that medium scale turbulence in the surface layer is approximately normally distributed except under very stable conditions. Also, Deardorff and Willis(18) conducted experiments showing that elevated maximums, not

TABLE 1

VERTICAL DISPERSION PARAMETER (SIGMA Z)
 CALCULATED FROM GROUND LEVEL SF6 CONCENTRATIONS
 GENERAL MOTORS SULFATE EXPERIMENT DATA

RUN NO.	SIGMA Z (METERS)					U (M/S)	PHI (DEG)	STAB
	2M (DOWNWIND FROM EDGE OF MIXING CELL)	15M	30M	50M	100M			
3030839	4.0	9.8	26.3	38.3	55.2	1.0	9	B
2750909	2.2	3.9	7.0	12.5	21.7	2.2	19	B
2750939	1.8	3.3	3.5	10.3	23.4	2.4	15	B
3000900	2.0	3.4	5.9	6.9	15.2	2.4	19	C
3020904	1.5	3.6	6.7	12.1	24.4	2.9	8	C
3020934	1.9	5.8	11.5	25.5	71.9	3.1	6	C
3020834	1.7	3.6	6.0	9.5	17.0	2.6	8	D
2860845	1.8	3.1	3.8	6.7	11.1	2.4	15	E
3000800	2.4	4.2	5.2	6.7	13.4	1.8	14	F
2860815	1.9	3.1	5.0	7.4	14.8	2.3	7	F
2970804	.7	2.0	3.8	7.4	35.1	2.5	2	F
2970834	1.1	2.2	4.2	4.5	29.4	2.2	3	F
3020804	2.0	3.1	5.2	7.7	14.2	1.8	14	F
2960805	1.0	2.2	4.2	8.0	26.6	2.9	1	F
2960834	1.1	1.7	3.6	7.4	39.9	3.0	3	F
2830950	3.3	5.3	8.1	----	25.6	1.3	40	B
2760914	1.9	2.7	3.3	5.1	10.0	2.7	47	B
2940935	2.6	3.8	5.8	8.4	14.6	1.4	39	B
3000930	2.1	3.8	5.8	9.8	16.8	2.2	21	B
2760944	1.8	3.0	4.1	5.6	8.1	3.1	56	B
2741540	2.1	3.0	5.1	8.1	14.3	3.0	68	B
2741510	2.6	3.7	6.3	8.4	11.5	2.8	69	B
2940905	2.8	4.4	7.2	9.7	18.5	1.1	30	C
2741440	2.1	3.8	6.8	7.0	15.0	2.6	68	C
3000830	2.1	2.8	4.7	6.9	11.9	2.3	20	C
2860945	1.8	3.1	3.8	5.6	11.1	2.9	22	C
2830920	4.2	5.3	7.7	10.5	16.8	1.1	62	C
2750809	4.3	8.0	23.0	15.0	28.9	.9	39	F
2790840	2.7	4.6	6.5	8.1	10.3	1.0	67	F
2760814	1.5	2.1	3.6	5.4	8.0	2.3	29	F
2750839	2.5	4.6	7.7	10.3	17.6	1.6	25	F
2940805	2.4	2.9	4.2	5.7	8.6	1.6	50	F
2940835	2.4	3.8	4.9	6.7	9.0	1.5	55	F
2790939	2.6	4.0	5.6	8.0	14.5	1.8	70	B
2830850	4.1	6.0	10.3	13.9	26.6	1.0	83	C
2790909	2.9	3.9	5.7	7.4	15.0	1.4	73	C
2931100	2.9	4.4	4.9	7.8	12.9	2.1	89	C
2931030	3.3	4.0	6.2	9.8	14.4	2.0	88	D
2830819	3.3	5.1	6.8	8.9	17.3	1.2	74	E
2790809	3.2	4.5	6.0	7.7	10.6	1.0	71	F

TABLE 2

VERTICAL DISPERSION PARAMETER (SIGMA Z)
 CALCULATED FROM GROUND LEVEL CO CONCENTRATIONS
 STANFORD RESEARCH INSTITUTE AT-GRADE SITE DATA

DATE-TIME	SIGMA Z (METERS)							U (M/S)	PHI (DEG)	STAB
	6M (DOWNWIND FROM EDGE OF MIXING CELL)	20M	46M	61M	76M	92M				
5 FEB 1200	2.0	3.3	5.3	7.4	9.2	12.3	2.5	46	B	
5 FEB 1300	1.6	2.5	4.6	4.0	5.5	6.9	3.5	63	B	
5 FEB 1400	1.7	2.5	4.0	4.4	5.1	5.9	3.0	67	B	
28 JAN 1000	2.3	4.2	---	8.4	8.4	14.0	2.1	32	D	
28 JAN 0700	1.0	1.8	2.8	2.6	---	3.6	2.9	46	D	
28 JAN 0900	1.3	2.6	---	---	8.4	6.7	2.8	51	D	
28 JAN 0800	1.0	1.7	2.0	2.2	---	4.1	3.2	55	D	
5 FEB 1800	2.9	4.3	6.7	---	8.1	---	1.3	55	D	
5 FEB 1700	2.8	3.4	5.0	6.2	---	6.6	2.3	69	D	
5 FEB 1500	1.3	1.5	3.9	5.0	3.5	5.0	4.2	72	D	
5 FEB 1600	2.0	2.7	3.9	4.8	---	5.5	3.5	72	D	
21 JAN 0600	3.3	5.3	5.3	7.7	---	9.4	.7	9	F	
28 JAN 0500	.7	---	1.8	3.7	---	---	2.4	25	F	
28 JAN 0600	1.9	---	4.3	4.7	---	4.3	2.5	32	F	
24 JAN 0700	1.6	3.0	3.0	4.9	---	6.8	1.4	37	F	
24 JAN 0600	2.7	5.1	5.3	8.6	---	9.3	1.1	44	F	
21 JAN 0700	3.5	6.2	7.0	8.1	8.6	7.3	.6	46	F	
24 JAN 0800	5.0	9.8	---	14.2	34.8	11.6	.5	47	F	
30 JAN 1900	5.1	7.1	10.6	10.6	18.2	21.3	.5	87	F	
24 JAN 1200	1.7	3.1	5.6	---	8.4	8.4	1.9	44	B	
30 JAN 1400	2.7	5.5	---	13.7	---	---	1.9	49	B	
30 JAN 1500	1.6	2.2	4.6	---	7.9	---	2.7	50	B	
24 JAN 1100	2.2	3.9	5.3	---	13.9	8.7	1.4	56	B	
30 JAN 1600	1.1	2.2	3.8	4.4	4.8	5.7	2.3	66	B	
21 JAN 0900	1.8	4.8	---	8.6	9.5	---	1.1	79	B	
30 JAN 1800	1.6	2.2	3.4	3.0	3.2	3.4	1.6	40	D	
30 JAN 1700	1.4	2.5	4.5	4.2	5.4	6.2	1.8	56	D	

TABLE 3

VERTICAL DISPERSION PARAMETER (SIGMA Z)
 CALCULATED FROM GROUND LEVEL SF6 CONCENTRATIONS
 NEW YORK "ROAD" PROJECT DATA

RUN NO.	SIGMA Z (METERS)				U (M/S)	PHI (DEG)	STAB
	4M (DOWNWIND OF MIXING CELL)	24M	40M	58M			
1005R1	2.0	6.3	8.9	12.8	3.6	9	C
1005R2	2.0	4.8	5.6	7.9	3.1	16	B
1006R1	2.9	---	---	---	2.1	25	B
1006R2	3.9	5.7	8.7	11.0	1.8	76	D
1007R1	2.0	3.2	5.2	8.0	3.6	7	B
1007R2	2.0	5.3	5.8	10.2	2.3	22	B
1008R1	2.9	6.7	8.4	10.4	2.5	64	B
1018R1	2.0	3.9	6.0	5.0	4.6	80	C
1019R1	4.9	7.2	6.1	4.5	1.3	57	B
1019R2	5.1	9.7	15.0	17.9	1.9	74	B
1019R3	5.1	6.2	8.6	12.4	1.8	66	C
1020R1	6.5	12.8	19.3	24.6	1.0	24	B
1021R1	1.9	2.0	2.7	4.3	7.5	48	D
1021R2	2.0	4.4	6.6	8.9	6.0	48	C
1115R1	4.1	10.5	16.9	19.6	2.0	14	C
1116R1	2.0	5.8	7.1	8.3	5.0	59	B
1116R2	2.0	4.3	5.5	6.6	5.0	76	B
1116R3	6.9	---	11.1	10.3	.9	75	F
1117R1	3.9	8.0	10.8	12.5	3.4	14	D
1118R1	3.7	7.5	8.3	10.5	6.5	65	D
1118R2	---	7.8	9.9	10.3	6.8	70	D

TABLE 4

BEST FIT GAUSSIAN DISTRIBUTION
 GM SULFATE EXPERIMENT TRACER MEASUREMENTS (SF6 IN PPFB)
 TOWER 4 (2 METERS DOWNWIND)

RUN NO.	* *	SIGMA Z (M)	YHAT-Y (PPFB)			* *	U (M/S)	PHI (DEG)	STAB
			0.5M	3.5M	9.5M				
3030839	*	4.4	-22	11	-52	*	1.0	9	B
2750909	*	2.2	-7	-15	-12	*	2.2	19	B
2750939	*	2.0	-20	-39	-17	*	2.4	15	B
3000900	*	2.4	-43	-98	-36	*	2.4	19	C
3020904	*	1.9	-47	-97	-70	*	2.9	8	C
3020934	*	2.1	-26	-52	-49	*	3.1	6	C
3020834	*	2.1	-42	-87	-46	*	2.6	8	D
2860845	*	2.0	-31	-61	-24	*	2.4	15	E
3000800	*	2.7	-23	-67	-39	*	1.8	14	F
2860815	*	2.2	-36	-77	-61	*	2.3	7	F
2970804	*	.9	-147	-216	-122	*	2.5	2	F
2970834	*	1.0	-12	-245	-131	*	2.2	3	F
3020804	*	2.1	-30	-62	-32	*	1.8	14	F
2960805	*	.9	-14	-193	-103	*	2.9	1	F
2960834	*	.9	-6	-226	99	*	3.0	3	F
2830950	*	3.4	-7	-15	-43	*	1.3	40	B
2760914	*	2.1	-25	-51	-10	*	2.7	47	B
2940935	*	2.7	-12	-32	-24	*	1.4	39	B
3000930	*	2.4	-33	-74	-30	*	2.2	21	B
2760944	*	1.9	-14	-29	-7	*	3.1	56	B
2741540	*	2.1	-1	-1	-11	*	3.0	68	B
2741510	*	2.5	3	9	-7	*	2.8	69	B
2940905	*	2.9	-11	-36	-39	*	1.1	30	C
2741440	*	2.1	30	1	-9	*	2.6	68	C
3000830	*	2.5	-33	-81	-27	*	2.3	20	C
2860945	*	2.1	-33	-66	-15	*	2.9	22	C
2830920	*	4.4	-8	22	-6	*	1.1	62	C
2750809	*	4.6	-17	65	10	*	.9	39	F
2790840	*	2.7	-4	-11	-12	*	1.0	67	F
2760814	*	1.8	-51	-104	-31	*	2.3	29	F
2750839	*	2.5	1	5	-13	*	1.6	25	F
2940805	*	2.5	-18	-45	-15	*	1.6	50	F
2940835	*	2.5	-13	-31	-13	*	1.5	55	F
2790939	*	2.5	-0	0	-2	*	1.8	70	B
2830850	*	4.1	-4	26	5	*	1.0	83	C
2790909	*	2.8	3	12	-4	*	1.4	73	C
2931100	*	2.8	6	23	-1	*	2.1	89	C
2931030	*	3.2	1	14	1	*	2.0	88	D
2830819	*	3.3	0	6	-1	*	1.2	74	E
2790809	*	3.2	-2	-1	-12	*	1.0	71	F

TABLE 5

BEST FIT GAUSSIAN DISTRIBUTION
 GM SULFATE EXPERIMENT TRACER MEASUREMENTS (SF6 IN PPHB)
 TOWER 5 (15 METERS DOWNWIND)

RUN NO.	* *	SIGMA Z (M)	YHAT-Y (PPHB)			* *	U (M/S)	PHI (DEG)	STAB
			0.5M	3.5M	9.5M				
3030839	*	9.7	1	-1	-10	*	1.0	9	B
2750909	*	4.2	-8	11	-16	*	2.2	19	B
2750939	*	3.3	-3	-3	-18	*	2.4	15	B
3000900	*	3.6	-8	-28	-45	*	2.4	19	C
3020904	*	4.0	-11	-28	-56	*	2.9	8	C
3020934	*	6.2	-3	-7	-17	*	3.1	6	C
3020834	*	4.0	-11	-23	-53	*	2.6	8	D
2860845	*	3.2	-7	-27	-40	*	2.4	15	E
3000800	*	4.5	-9	-23	-42	*	1.8	14	F
2860815	*	3.4	-11	-47	-63	*	2.3	7	F
2970804	*	2.6	-39	-103	-112	*	2.5	2	F
2970834	*	2.6	-37	-104	-108	*	2.2	3	F
3020804	*	3.3	-8	-24	-49	*	1.8	14	F
2960805	*	2.7	-34	-97	-109	*	2.9	1	F
2960834	*	2.3	-54	-120	-117	*	3.0	3	F
2830950	*	5.6	-7	-5	-22	*	1.3	40	B
2760914	*	2.8	-10	-35	-15	*	2.7	47	B
2940935	*	4.0	-11	-44	-62	*	1.4	39	B
3000930	*	4.0	-6	-22	-34	*	2.2	21	B
2760944	*	3.1	-4	-21	-6	*	3.1	56	B
2741540	*	3.0	0	6	-13	*	3.0	68	B
2741510	*	3.7	-2	-6	-8	*	2.8	69	B
2940905	*	4.7	-13	-23	-52	*	1.1	30	C
2741440	*	3.8	-3	2	-9	*	2.6	68	C
3000830	*	3.0	-8	-26	-41	*	2.3	20	C
2860945	*	3.2	-5	-19	-26	*	2.9	22	C
2830920	*	5.5	-6	6	-5	*	1.1	62	C
2750809	*	8.2	-5	16	42	*	.9	39	F
2790840	*	4.4	7	-22	3	*	1.0	67	F
2760814	*	2.4	-31	-74	-44	*	2.3	29	F
2750839	*	4.6	-1	-12	-12	*	1.6	25	F
2940805	*	3.0	-9	-37	-31	*	1.6	50	F
2790939	*	3.9	0	-6	-2	*	1.8	70	B
2830850	*	6.4	-9	24	12	*	1.0	83	C
2790909	*	4.1	-8	4	-23	*	1.4	73	C
2931100	*	4.4	-1	7	5	*	2.1	89	C
2931030	*	4.2	-6	35	3	*	2.0	88	D
2830819	*	5.2	-4	18	8	*	1.2	74	E
2790809	*	4.6	-4	-10	-19	*	1.0	71	F

TABLE 6

BEST FIT GAUSSIAN DISTRIBUTION
 GM SULFATE EXPERIMENT TRACER MEASUREMENTS (SF6 IN PPHB)
 TOWER 6 (30 METERS DOWNWIND)

RUN NO.	* *	SIGMA Z (M)	YHAT-Y (PPHB)			* *	U (M/S)	PHI (DEG)	STAB
			0.5M	3.5M	9.5M				
3030839	*	23.5	5	2	-8	*	1.0	9	B
2750909	*	7.3	-2	2	-4	*	2.2	19	B
2750939	*	3.6	-5	20	-21	*	2.4	15	B
3000900	*	6.0	-2	-12	-19	*	2.4	19	C
3020904	*	7.2	-4	-6	-26	*	2.9	8	C
3020934	*	11.7	-1	1	-2	*	3.1	6	C
3020834	*	6.8	-7	-6	-30	*	2.6	8	D
2860845	*	4.1	-8	-18	-38	*	2.4	15	E
3000800	*	5.8	-12	-11	-41	*	1.8	14	F
2860815	*	5.6	-8	-15	-35	*	2.3	7	F
2970804	*	4.5	-15	-36	-68	*	2.5	2	F
2970834	*	5.1	-17	-31	-68	*	2.2	3	F
3020804	*	5.6	-9	-6	-27	*	1.8	14	F
2960805	*	4.9	-13	-31	-58	*	2.9	1	F
2960834	*	4.5	-20	-26	-73	*	3.0	3	F
2830950	*	8.6	-5	7	1	*	1.3	40	B
2760914	*	3.4	-4	-11	-27	*	2.7	47	B
2940935	*	6.1	-7	-6	-24	*	1.4	39	B
3000930	*	6.6	-9	2	-21	*	2.2	21	B
2760944	*	4.2	-3	2	-6	*	3.1	56	B
2741540	*	5.3	-3	8	1	*	3.0	68	B
2741510	*	6.5	-3	6	4	*	2.8	69	B
2940905	*	7.1	2	-8	-11	*	1.1	30	C
2741440	*	6.3	4	-3	7	*	2.6	68	C
3000830	*	5.1	-8	-11	-29	*	2.3	20	C
2860945	*	4.1	-8	-9	-30	*	2.9	22	C
2830920	*	8.0	-4	9	14	*	1.1	62	C
2750809	*	17.9	14	-26	17	*	.9	39	F
2790840	*	6.4	1	1	4	*	1.0	67	F
2760814	*	3.9	-9	-30	-52	*	2.3	29	F
2750839	*	8.2	-4	7	3	*	1.6	25	F
2940805	*	4.4	-9	-5	-27	*	1.6	50	F
2940835	*	5.2	-9	10	-9	*	1.5	55	F
2790939	*	5.6	1	6	8	*	1.8	70	B
2830850	*	10.2	2	-4	17	*	1.0	83	C
2790909	*	5.7	0	-3	-3	*	1.4	73	C
2931100	*	5.4	-11	23	1	*	2.1	89	C
2931030	*	6.5	-4	16	14	*	2.0	88	D
2830819	*	7.1	-5	14	14	*	1.2	74	E
2790809	*	6.0	-1	-6	-8	*	1.0	71	F

TABLE 7

BEST FIT GAUSSIAN DISTRIBUTION
 SRI AT-GRADE SITE (CO IN PPM)
 TOWER 2 OR 4 (10.7 METERS DOWNWIND FROM EDGE OF ROADWAY)

DATE-TIME	*	SIGMA Z (M)	YHAT-Y (PPM)				*	U (M/S)	PHI (DEG)	STAB
			0.0M	3.0M	6.1M	13.6M				
5 FEB 1200	*	2.9	-.2	-.6	-.6	-.1	2.5	46	B	
5 FEB 1300	*	2.4	-.2	-.6	-.5	.0	3.5	63	B	
5 FEB 1400	*	2.6	-.3	-.7	-.6	-.2	3.0	67	B	
28 JAN 1000	*	3.8	-.1	-.5	-.5	-.3	2.1	32	D	
28 JAN 0700	*	1.9	-1.9	-2.8	-1.8	-.1	2.9	46	D	
28 JAN 0900	*	3.9	----	-1.3	-.9	-.2	2.8	51	D	
5 FEB 1800	*	3.8	-.1	-.3	-.3	-.2	1.3	55	D	
5 FEB 1700	*	3.1	-.4	-.9	-.9	-.3	2.3	69	D	
5 FEB 1500	*	1.9	-.7	-.6	-.8	----	4.1	72	D	
5 FEB 1600	*	2.6	-.4	-.7	-1.0	-.2	3.5	72	D	
28 JAN 0500	*	2.6	-.4	-1.5	-.4	-.8	2.4	25	F	
28 JAN 0600	*	3.9	-.4	----	-.9	-.3	2.5	32	F	
24 JAN 0700	*	3.1	-.7	-4.0	-2.0	-1.4	1.4	37	F	
24 JAN 0600	*	3.6	-.3	-.7	-.9	-.3	1.1	44	F	
21 JAN 0700	*	4.7	-1.2	----	-2.8	-3.2	.6	46	F	
24 JAN 0800	*	13.5	2.3	-1.3	-1.6	-.3	.5	47	F	
30 JAN 1900	*	5.8	.0	-.2	-.2	-.3	.5	87	F	
24 JAN 1200	*	3.0	-.4	-1.4	-1.0	-.4	1.9	44	B	
30 JAN 1400	*	3.8	-.1	-.2	-.3	-.4	1.9	49	B	
30 JAN 1500	*	2.1	-1.0	-2.3	-1.3	----	2.7	50	B	
30 JAN 1600	*	2.0	-1.4	-3.1	-1.3	-.1	2.3	66	B	
21 JAN 0900	*	4.4	-.2	-.7	-1.3	-.9	1.1	79	B	
30 JAN 1700	*	2.2	-1.7	-4.0	-2.0	----	1.8	56	D	

TABLE 8

BEST FIT GAUSSIAN DISTRIBUTION
 SRI AT-GRADE SITE (CO IN PPM)
 TOWER 1 OR 5 (30.5 METERS DOWNWIND FROM EDGE OF ROADWAY)

DATE-TIME	*	SIGMA Z (M)	YHAT-Y (PPM)				*	U (M/S)	PHI (DEG)	STAB
			0.0M	3.0M	6.1M	13.6M				
5 FEB 1200	*	3.9	.0	-.2	----	-.3	* 2.5	46	B	
5 FEB 1300	*	3.7	-.1	-.2	-.2	.0	* 3.5	63	B	
5 FEB 1400	*	3.5	-.2	-.3	-.5	----	* 3.0	67	B	
28 JAN 1000	*	5.5	-.0	-.1	-.4	-.3	* 2.1	32	D	
28 JAN 0700	*	2.5	-.3	-1.4	----	-.3	* 2.9	46	D	
28 JAN 0900	*	3.6	-.2	-.5	-.6	----	* 2.8	51	D	
28 JAN 0800	*	2.7	-.5	-1.4	-1.0	-.3	* 3.2	55	D	
5 FEB 1800	*	3.2	-.2	.4	-.3	.0	* 1.3	55	D	
5 FEB 1700	*	4.4	.0	-.5	-.5	----	* 2.3	69	D	
5 FEB 1500	*	3.8	-.2	-.3	-.6	-.6	* 4.1	72	D	
5 FEB 1600	*	3.5	-.2	-.6	-.7	-.3	* 3.5	72	D	
21 JAN 0600	*	7.6	-.4	----	-.6	-1.2	* .7	9	F	
28 JAN 0500	*	3.5	-.3	----	-.6	-.1	* 2.4	25	F	
28 JAN 0600	*	2.0	-.5	-1.3	----	-.4	* 2.5	32	F	
24 JAN 0700	*	4.5	-.1	-.9	-1.6	----	* 1.4	37	F	
24 JAN 0600	*	6.9	.3	-.5	-.2	-.3	* 1.1	44	F	
21 JAN 0700	*	7.0	-.5	----	.0	-1.2	* .6	46	F	
24 JAN 0800	*	8.7	.3	-.9	.1	-1.0	* .5	47	F	
30 JAN 1900	*	9.6	-.2	.2	.1	.1	* .5	87	F	
24 JAN 1200	*	4.7	-.1	-.0	-.5	----	* 1.9	44	B	
30 JAN 1400	*	9.5	-.0	-.0	-.0	-.2	* 1.9	49	B	
24 JAN 1100	*	4.9	.1	-.8	-1.2	----	* 1.4	56	B	
30 JAN 1600	*	4.1	----	-1.1	-1.0	-.2	* 2.3	66	B	
21 JAN 0900	*	7.4	.2	-.4	-.2	-.5	* 1.1	79	B	
30 JAN 1800	*	4.2	----	-1.0	-.9	-.5	* 1.6	40	D	

BEST FIT GAUSSIAN DISTRIBUTION
 NEW YORK DATA (SF6 IN PPHB)
 TOWER 5 OR 9 (4 METERS DOWNWIND FROM EDGE OF ROADWAY)

RUN NO.*	* SIGMA		YHAT-Y (PPHB)				* U	PHI	STAR	
	* Z (M)		2.0M	4.0M	8.0M	16.0M				* (M/S)
1005R1	*	3.4	-198	-214	-230	-170	*	3.6	9	C
1005R2	*	3.8	-154	-229	-211	-70	*	3.1	16	B
1006R1	*	3.7	-113	-65	-175	-120	*	2.1	25	B
1006R2	*	4.1	-16	27	-24	-20	*	1.8	76	D
1007R1	*	3.0	-327	-336	-236	-80	*	3.6	7	B
1007R2	*	3.6	-179	-242	-224	-70	*	2.3	22	B
1008R1	*	3.4	-50	-39	-69	-10	*	2.5	64	B
1018R1	*	2.5	-65	-32	-28	-10	*	4.6	80	C
1019R1	*	1.1	5	----	-640	-520	*	1.3	57	B
1019R2	*	1.1	23	-395	-120	-20	*	1.9	74	B
1019R3	*	1.1	19	-344	-130	-40	*	1.8	66	C
1020R1	*	1.0	21	-697	-490	-230	*	1.0	24	B
1021R1	*	2.8	-162	-135	-56	-10	*	7.5	48	D
1021R2	*	2.7	-157	-114	-85	----	*	6.0	48	C
1115R1	*	4.4	-26	5	-38	-49	*	2.0	14	C
1116R1	*	2.7	-36	-22	-35	-3	*	5.0	59	B
1116R2	*	2.9	-118	-112	-61	-10	*	5.0	76	B
1116R3	*	1.0	29	-617	-170	-7	*	.9	75	F
1117R1	*	4.1	-14	9	-20	----	*	3.4	14	D
1118R1	*	3.6	4	18	0	-3	*	6.5	65	D
1118R2	*	3.4	----	8	-6	-3	*	6.8	70	D

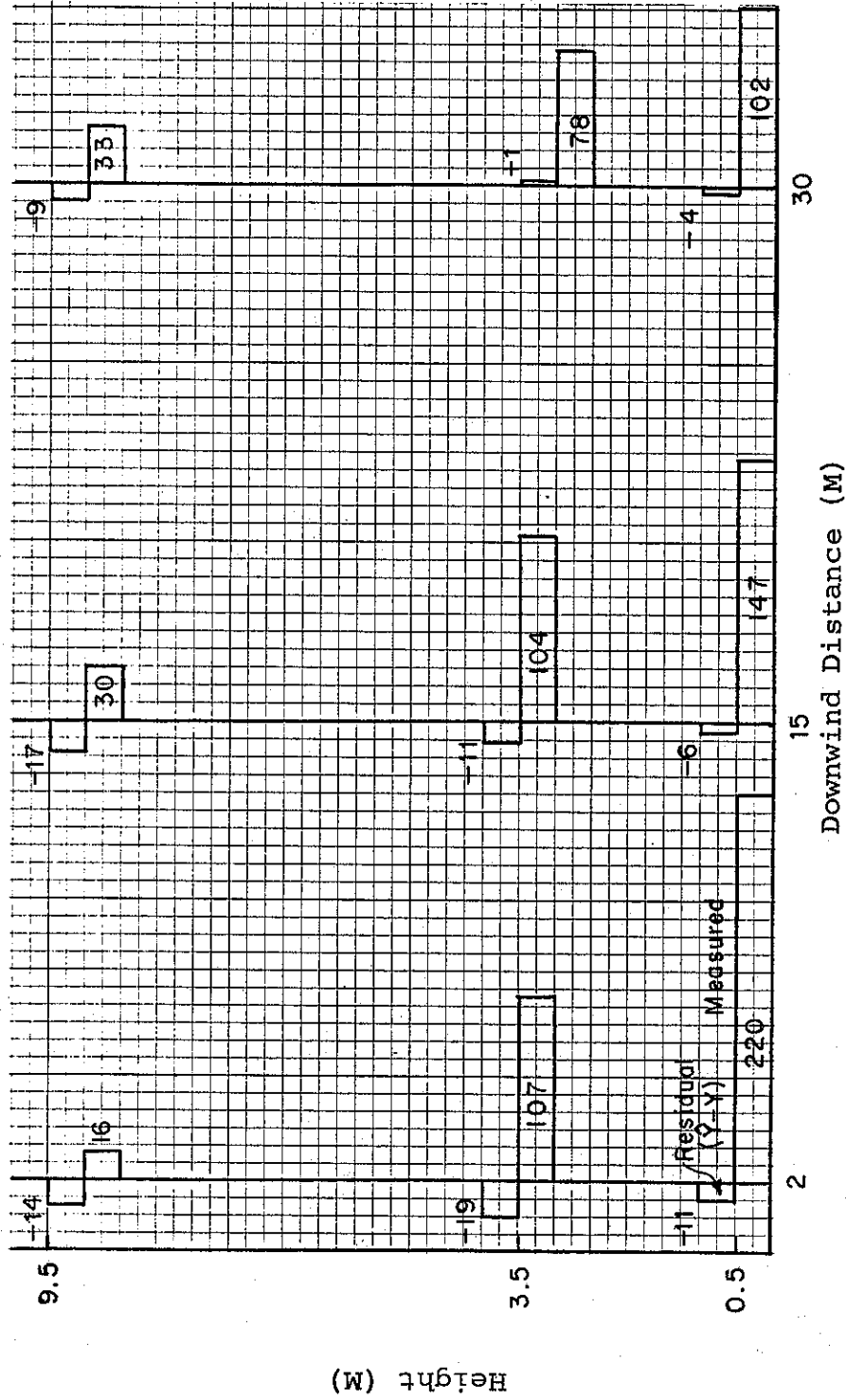


Fig. 6 Average Measured and Residual ($\hat{Y}-Y$) SF₆ Concentrations (PPHB) for $\phi \geq 20^\circ$, $u \geq 1.0$ M/S, GM Data (22 Cases)

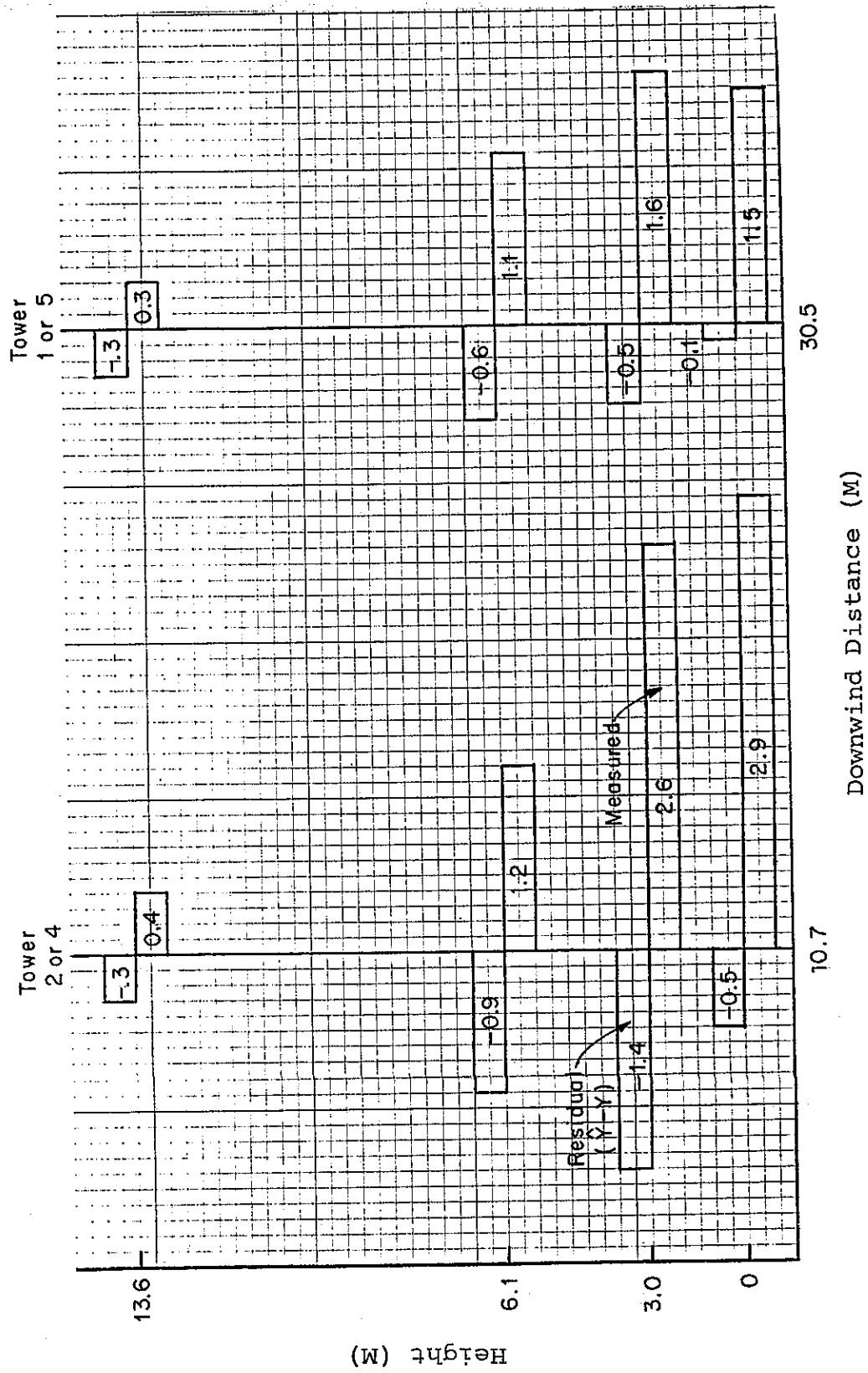


Fig. 7 Average Measured and Residual ($\hat{Y}-Y$) CO Concentrations (PPM) for $\Phi \approx 20^\circ$; $U \approx 1.0$ M/S, SRI Data (21 Cases)

apparent in these data, require sufficient downstream distance to form, and that within the ranges examined in this report the Gaussian assumption of normality is valid. This leaves source strength as the suspect variable.

A study of the spatial distribution of the residuals is particularly revealing and leads to a possible explanation of the results. In general, the residuals get smaller as distance from the source increases. Also, the ground level residuals are consistently smaller than the values at higher levels. This behavior in the residuals could be explained by the existence of an interfering compound uniformly distributed upwind of the source and reacting with automobile exhaust constituents downwind of the source. (Note that the SRI CO source strength is normalized by tracer results.) Another interesting observation is the progressively larger negative residuals (as compared to observed concentrations) for the GM, SRI, and NY data bases, respectively (see Table 9 for NY residuals). This could represent site to site differences in the ambient level of the hypothesized interfering compound.

Typical ambient levels of SF₆ (used as the tracer in all three studies) are reported to be less than 0.02 PPHB(19). This is totally insignificant when compared to the observed residuals. In fact Dietz and Cote(20) have reported significant SF₆ absorption on teflon which would lead to positive rather than negative residuals. All three field studies were designed to minimize this absorption problem.

No reference in the literature could be found which described compounds that interfere with SF₆ test results. It is suggested that interference might be a problem and that further research is needed in this area.

As regards the σ_z tower measurements, their reliability is reasonably independent of this type of systematic error because of the least squares fitting technique. However, σ_z estimates based on ground level results are directly related to the source strength - measured concentration ratio. For both the SRI and NY data, the large negative ground level residuals make this ratio unreliable. Therefore, only the tower data and GM ground level results will be used to determine the recommended σ_z curves.

Another very plausible explanation for the negative residuals involves the wind direction with respect to the highway. Study of the GM results (Tables 4 thru 6) shows a correlation between the frequency and size of the negative residuals and the wind angle (PHI). As the wind direction approaches parallel to the freeway (PHI \rightarrow 0) the negative residuals increase. This could be attributed to a longer fetch over the source (important for receptors close to the line source). A factor of $1/\sin\phi$ was applied to the P-normal equation to adjust for the longer fetch. Best fit σ_z values were computed for the GM and SRI data (Tables 10 thru 14). An examination of the GM residuals shows a more favorable balance with a tendency toward overprediction, i.e., positive residuals (possibly explained by SF₆ absorption in the sampling train), and a more peaked distribution than the Gaussian function predicts. However there are still systematic differences in the residuals as a function of PHI, and the SRI data still yields systematically negative residuals. As a result of this confusion, the recommended σ_z curves were only based on measurements taken when PHI \geq 45°.

TABLE 10

BEST FIT GAUSSIAN DISTRIBUTION
 GM SULFATE EXPERIMENT TRACER MEASUREMENTS (SF6 IN PPHB)
 TOWER 4 (2 METERS DOWNWIND)

RUN NO.	* *	SIGMA Z (M)	YHAT-Y (PPHB)			* *	U (M/S)	PHI (DEG)	STAB
			0.5M	3.5M	9.5M				
3030839	*	40.8	-89	7	90	*	1.0	9	B
2750909	*	8.8	-44	65	69	*	2.2	19	B
2750939	*	9.9	-54	60	77	*	2.4	15	B
3000900	*	6.0	-4	27	27	*	2.4	19	C
3020904	*	14.7	-62	33	65	*	2.9	8	C
3020934	*	29.7	-65	18	56	*	3.1	6	C
3020834	*	17.6	-72	20	87	*	2.6	8	D
2860845	*	7.8	-32	64	64	*	2.4	15	E
3000800	*	12.6	-53	22	103	*	1.8	14	F
2860815	*	22.5	-69	15	73	*	2.3	7	F
2970804	*	33.0	-204	70	154	*	2.5	2	F
2970834	*	27.1	-105	12	113	*	2.2	3	F
3020804	*	10.7	-74	68	109	*	1.8	14	F
2960805	*	67.3	-135	26	113	*	2.9	1	F
2960834	*	44.9	-173	-67	255	*	3.0	3	F
2830950	*	5.4	-14	26	-4	*	1.3	40	B
2760914	*	2.6	-6	-16	-10	*	2.7	47	B
2940935	*	4.3	-12	49	-0	*	1.4	39	B
3000930	*	5.9	-11	42	30	*	2.2	21	B
2760944	*	2.2	-5	-11	-7	*	3.1	56	B
2741540	*	2.2	2	6	-11	*	3.0	68	B
2741510	*	2.7	5	16	-7	*	2.8	69	B
2940905	*	6.1	-19	71	50	*	1.1	30	C
2741440	*	2.2	4	10	-9	*	2.6	68	C
3000830	*	6.2	-3	32	37	*	2.3	20	C
2860945	*	4.8	-8	33	10	*	2.9	22	C
2830920	*	5.0	-10	31	8	*	1.1	62	C
2750809	*	8.2	-44	80	92	*	.9	39	F
2790840	*	2.9	1	8	-11	*	1.0	67	F
2760814	*	3.1	-2	11	-28	*	2.3	29	F
2750839	*	7.4	-41	88	69	*	1.6	25	F
2940805	*	3.1	-1	3	-12	*	1.6	50	F
2940835	*	2.9	1	7	-12	*	1.5	55	F
2790939	*	2.6	2	8	-2	*	1.8	70	B
2830850	*	4.2	-5	27	5	*	1.0	83	C
2790909	*	2.9	4	19	-4	*	1.4	73	C
2931100	*	2.8	6	23	-1	*	2.1	89	C
2931030	*	3.2	1	14	1	*	2.0	88	D
2830819	*	3.4	0	11	-0	*	1.2	74	E
2790809	*	3.4	-1	9	-10	*	1.0	71	F

TABLE 11

BEST FIT GAUSSIAN DISTRIBUTION
 GM SULFATE EXPERIMENT TRACER MEASUREMENTS (SF6 IN PPHB)
 TOWER 5 (15 METERS DOWNWIND)

RUN NO.	* *	SIGMA Z (M)	YHAT-Y (PPHB)			* *	U (M/S)	PHI (DEG)	STAB
			0.5M	3.5M	9.5M				
3030839	*	71.9	-11	-7	18	*	1.0	9	B
2750909	*	17.9	-35	11	38	*	2.2	19	B
2750939	*	19.4	-38	7	47	*	2.4	15	B
3000900	*	11.3	-13	7	33	*	2.4	19	C
3020904	*	28.8	-13	-3	19	*	2.9	8	C
3020934	*	69.4	-9	-4	13	*	3.1	6	C
3020834	*	30.6	-21	-2	26	*	2.6	8	D
2860845	*	14.2	-22	5	40	*	2.4	15	E
3000800	*	20.8	-27	-8	48	*	1.8	14	F
2860815	*	30.4	-22	-11	38	*	2.3	7	F
2970804	*	63.0	-28	-8	37	*	2.5	2	F
2970834	*	44.9	-31	-11	46	*	2.2	3	F
3020804	*	17.1	-44	9	60	*	1.8	14	F
2960805	*	102.5	-22	-11	33	*	2.9	1	F
2960834	*	43.4	-39	-2	44	*	3.0	3	F
2830950	*	8.5	-5	9	17	*	1.3	40	B
2760914	*	3.7	-2	-8	-11	*	2.7	47	B
2940935	*	6.1	-3	-7	-15	*	1.4	39	B
3000930	*	11.6	-13	4	39	*	2.2	21	B
2760944	*	3.6	-1	-8	-4	*	3.1	56	B
2741540	*	3.2	-0	12	-12	*	3.0	68	B
2741510	*	4.0	-1	-2	-6	*	2.8	69	B
2940905	*	9.3	-10	14	43	*	1.1	30	C
2741440	*	4.2	-3	6	-6	*	2.6	68	C
3000830	*	9.5	-22	27	41	*	2.3	20	C
2860945	*	8.9	-9	14	28	*	2.9	22	C
2830920	*	6.2	-4	13	8	*	1.1	62	C
2750809	*	16.4	-33	-3	64	*	.9	39	F
2790840	*	4.7	9	-14	11	*	1.0	67	F
2760814	*	4.5	-12	10	-22	*	2.3	29	F
2750839	*	12.8	-18	-1	56	*	1.6	25	F
2940805	*	3.9	-6	-1	-21	*	1.6	50	F
2790939	*	4.2	1	-2	1	*	1.8	70	B
2830850	*	6.4	-9	24	13	*	1.0	83	C
2790909	*	4.3	-9	7	-20	*	1.4	73	C
2931100	*	4.4	-1	7	5	*	2.1	89	C
2931030	*	4.2	-7	35	3	*	2.0	88	D
2830819	*	5.4	-4	20	12	*	1.2	74	E
2790809	*	4.8	-4	-5	-13	*	1.0	71	F

TABLE 12

BEST FIT GAUSSIAN DISTRIBUTION
 GM SULFATE EXPERIMENT TRACER MEASUREMENTS (SF6 IN PPHB)
 TOWER 6 (30 METERS DOWNWIND)

RUN NO.	* SIGMA * Z (M)	YHAT-Y (PPHB)			* U * (M/S)	PHI (DEG)	STAB
		0.5M	3.5M	9.5M			
3030839	* 157.4	4	1	-6	* 1.0	9	B
2750909	* 26.9	-12	-2	17	* 2.2	19	B
2750939	* 23.3	-44	18	34	* 2.4	15	B
3000900	* 19.4	-7	-7	20	* 2.4	19	C
3020904	* 49.4	-3	1	2	* 2.9	8	C
3020934	* 130.5	-3	-0	3	* 3.1	6	C
3020834	* 46.5	-7	2	5	* 2.6	8	D
2860845	* 17.1	-16	-0	28	* 2.4	15	E
3000800	* 24.7	-17	-1	22	* 1.8	14	F
2860815	* 46.6	-11	-5	17	* 2.3	7	F
2970804	* 105.7	-6	-7	12	* 2.5	2	F
2970834	* 77.1	-6	-3	9	* 2.2	3	F
3020804	* 26.2	-22	-2	29	* 1.8	14	F
2960805	* 181.6	-5	-7	13	* 2.9	1	F
2960834	* 81.7	-10	4	6	* 3.0	3	F
2830950	* 14.5	-12	4	18	* 1.3	40	B
2760914	* 4.7	-8	6	-14	* 2.7	47	B
2940935	* 9.5	-5	6	16	* 1.4	39	B
3000930	* 19.2	-14	6	13	* 2.2	21	B
2760944	* 5.1	-3	8	1	* 3.1	56	B
2741540	* 5.7	-3	9	5	* 3.0	68	B
2741510	* 7.0	-3	7	7	* 2.8	69	B
2940905	* 15.8	-11	-9	35	* 1.1	30	C
2741440	* 6.8	5	-1	11	* 2.6	68	C
3000830	* 15.7	-13	-0	24	* 2.3	20	C
2860945	* 11.3	-11	8	18	* 2.9	22	C
2830920	* 9.3	-7	9	22	* 1.1	62	C
2750809	* 29.5	11	-28	19	* .9	39	F
2790840	* 7.0	2	4	13	* 1.0	67	F
2760814	* 7.5	-3	2	-4	* 2.3	29	F
2750839	* 23.7	-17	-0	22	* 1.6	25	F
2940805	* 5.8	-7	10	-3	* 1.6	50	F
2940835	* 6.3	-8	19	9	* 1.5	55	F
2790939	* 5.9	1	8	12	* 1.8	70	B
2830850	* 10.2	1	-4	18	* 1.0	83	C
2790909	* 5.9	1	-1	0	* 1.4	73	C
2931100	* 5.4	-11	23	1	* 2.1	89	C
2931030	* 6.5	-4	16	14	* 2.0	88	D
2830819	* 7.4	-5	14	17	* 1.2	74	E
2790809	* 6.3	0	-3	-3	* 1.0	71	F

TABLE 13

BEST FIT GAUSSIAN DISTRIBUTION
 SRI AT-GRADE SITE (CO IN PPM)
 TOWER 2 OR 4 (10.7 METERS DOWNWIND FROM EDGE OF ROADWAY)

DATE-TIME	* SIGMA	YHAT-Y (PPM)				* U	PHI	STAB
	* Z (M)	0.0M	3.0M	6.1M	13.6M	* (M/S)	(DEG)	
5 FEB 1200	* 3.7	-.1	-.3	-.4	-.1	* 2.5	46	B
5 FEB 1300	* 2.7	-.2	-.4	-.4	.0	* 3.3	63	B
5 FEB 1400	* 2.7	-.3	-.6	-.6	-.2	* 2.9	67	B
28 JAN 1000	* 8.7	.1	-.1	.2	.1	* 1.5	32	D
28 JAN 0700	* 2.2	-.9	-2.0	-1.7	-.1	* 2.7	46	D
28 JAN 0900	* 4.0	----	-.9	-.7	-.2	* 2.4	51	D
5 FEB 1800	* 9.1	-.2	.0	.7	.4	* .7	55	D
5 FEB 1700	* 4.6	-.0	.1	.1	-.3	* 1.5	69	D
5 FEB 1500	* 1.9	-.6	-.6	-.8	----	* 4.2	72	D
5 FEB 1600	* 3.0	-.3	-.4	-.8	-.2	* 3.1	72	D
28 JAN 1100	* 27.0	-.2	----	-.0	.3	* .7	78	D
28 JAN 0500	* 3.3	.0	-1.2	-.3	-.8	* 2.4	25	F
28 JAN 0600	* 5.9	-.1	----	-.4	-.2	* 2.5	32	F
24 JAN 0700	* 4.7	.8	-2.0	-.1	-1.3	* 1.1	37	F
24 JAN 0600	* 4.5	-.0	-.2	-.3	-.3	* 1.2	44	F
21 JAN 0700	* 6.3	-.9	----	-1.4	-2.7	* .6	46	F
24 JAN 0800	* 21.2	2.4	-1.2	-1.5	.2	* .4	47	F
30 JAN 1900	* 11.9	-.1	-.0	.4	.7	* .3	87	F
24 JAN 1200	* 3.8	-.0	-.9	-.6	-.4	* 1.7	44	B
30 JAN 1400	* 5.9	-.1	-.0	.1	-.3	* 1.7	49	B
30 JAN 1500	* 2.6	-.6	-1.6	-1.1	----	* 2.5	50	B
30 JAN 1600	* 2.3	-1.0	-2.6	-1.2	-.1	* 2.2	66	B
21 JAN 0900	* 4.8	-.2	-.5	-1.1	-.9	* 1.0	79	B
30 JAN 1700	* 2.3	-1.4	-3.6	-1.9	----	* 1.9	56	D

TABLE 14

BEST FIT GAUSSIAN DISTRIBUTION
 SRI AT-GRADE SITE (CO IN PPM)
 TOWER 1 OR 5 (30.5 METERS DOWNWIND FROM EDGE OF ROADWAY)

DATE-TIME	* SIGMA	YHAT-Y (PPM)				* U	PHI	STAB
	* Z (M)	0.0M	3.0M	6.1M	13.6M	* (M/S)	(DEG)	
5 FEB 1200	* 5.7	.0	-.1	----	-.2	* 2.5	46	B
5 FEB 1300	* 4.2	-.0	-.1	-.1	.0	* 3.3	63	B
5 FEB 1400	* 3.7	-.1	-.2	-.4	----	* 2.9	67	B
28 JAN 1000	* 13.0	.0	.0	-.1	.2	* 1.5	32	D
28 JAN 0700	* 3.2	.0	-.7	----	-.3	* 2.7	46	D
28 JAN 0900	* 4.6	.0	-.3	-.3	----	* 2.4	51	D
28 JAN 0800	* 3.3	-.2	-1.0	-.8	-.3	* 2.8	55	D
5 FEB 1800	* 9.0	-.6	.7	.8	.6	* .7	55	D
5 FEB 1700	* 7.0	.1	-.2	.3	----	* 1.5	69	D
5 FEB 1500	* 3.8	-.2	-.3	-.5	-.6	* 4.2	72	D
5 FEB 1600	* 4.0	-.1	-.4	-.5	-.3	* 3.1	72	D
28 JAN 1100	* 39.3	.0	-.2	-.1	.2	* .7	78	D
21 JAN 0600	* 38.4	-.4	----	-.0	.5	* .9	9	F
28 JAN 0500	* 5.2	-.1	----	-.4	-.1	* 2.4	25	F
28 JAN 0600	* 3.1	.0	-.2	----	-.4	* 2.5	32	F
24 JAN 0700	* 8.0	.2	-.2	-.2	----	* 1.1	37	F
24 JAN 0600	* 9.0	.4	-.4	.0	.0	* 1.2	44	F
21 JAN 0700	* 9.5	-.4	----	.7	-.2	* .6	46	F
24 JAN 0800	* 13.7	.3	-.8	.6	.1	* .4	47	F
30 JAN 1900	* 22.3	-.4	.0	.1	.5	* .3	87	F
24 JAN 1200	* 6.9	-.1	.1	-.2	----	* 1.7	44	B
30 JAN 1400	* 14.4	-.0	-.0	.0	-.0	* 1.7	49	B
24 JAN 1100	* 5.8	.3	-.6	-.9	----	* 1.3	56	B
30 JAN 1600	* 4.2	----	-.8	-.8	-.2	* 2.2	66	B
21 JAN 0900	* 8.2	.2	-.4	-.1	-.4	* 1.0	79	B
30 JAN 1800	* 4.5	----	-.6	-.7	-.5	* 1.9	40	D

In the interest of further testing the validity of the Gaussian assumption near the freeway, GM observed and predicted (assuming a normal distribution) averages for $\text{PHI} \geq 70^\circ$ are plotted in Figure 8 (7 cases). Here a slight lack of fit is shown at the 3.5 meter height, but considering the expected irregular vertical distribution of mixing intensity near the freeway, the degree of fit to a normal distribution is remarkable. These results show that the Gaussian formulation can be used very near the freeway under crosswind conditions.

Figures 9 thru 12 graphically summarize the ground level and tower σ_z data for various atmospheric stability conditions. The appropriate σ_z curve presently used by CALINE2 is plotted on each graph. The error bars represent a \pm one standard deviation in the data. Despite the considerable scatter in the results, the expected overprediction of σ_z near the freeway by CALINE2 is apparent. Another significant feature of the graphs is that the σ_z values within 10 to 15 meters of the freeway appear to be independent of stability class. This would support the contention that very near the freeway, dispersion is dominated by traffic flow characteristics, not ambient atmospheric stability.

Best fit σ_z curves of the form $\sigma_z = \alpha x^\beta$, where x = downwind distance from the source in meters, were computed for each of the stability classes studied. In accordance with results from the residual analysis, the data were limited to tower results at 2, 10.7, 15, 30 and 30.5 meters for the GM and SRI studies, and ground level results at 50 and 100 meters for the GM study. Furthermore, conditions were restricted to $\phi \geq 45^\circ$ and $U \geq 1.0$ m/s. Table 15 give the resulting values of α and β for the

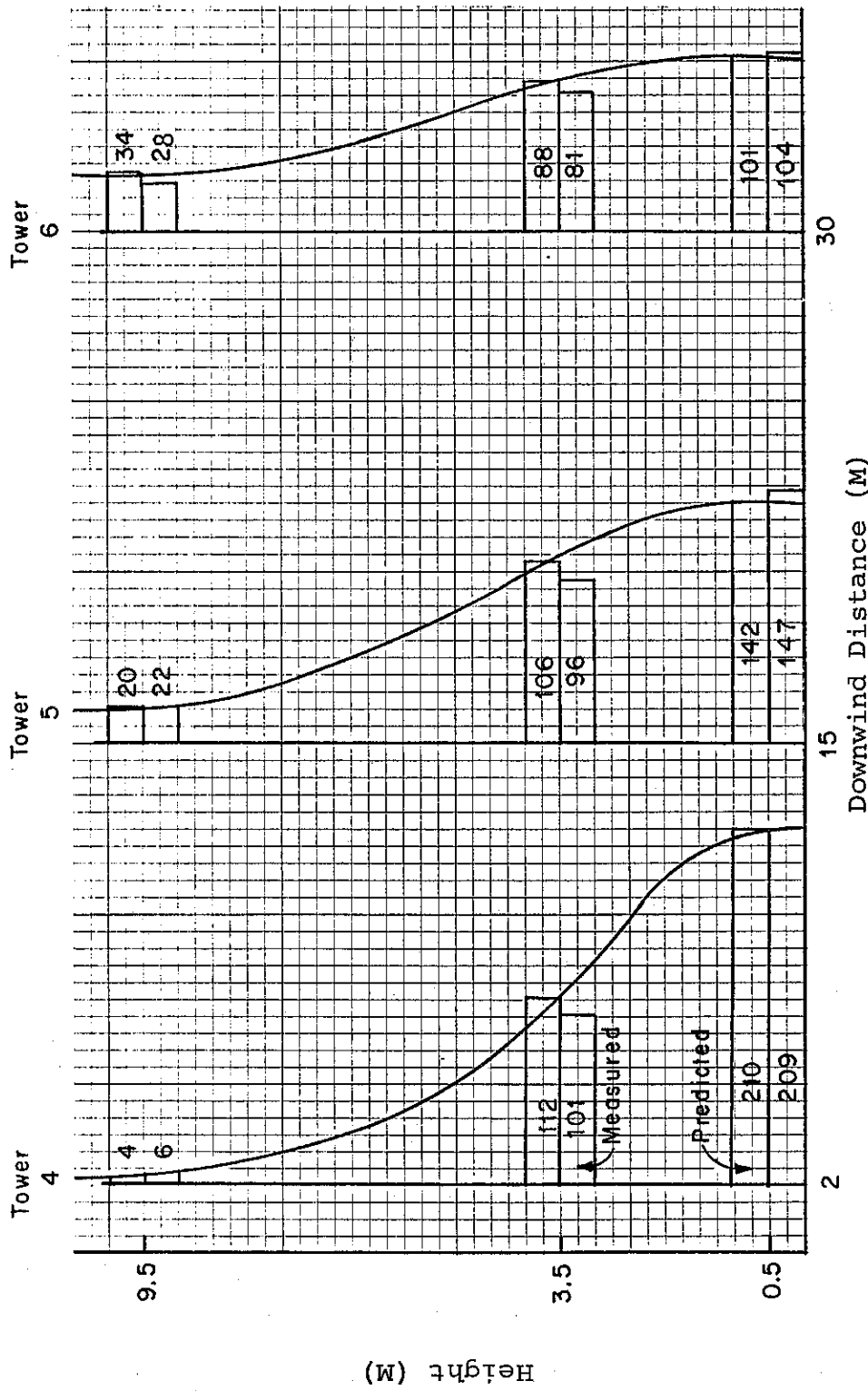


Fig. 8 Average Measured and Predicted SF6 Concentrations (PPHB) for $\phi \geq 70^\circ$; GM Data (7 Cases)

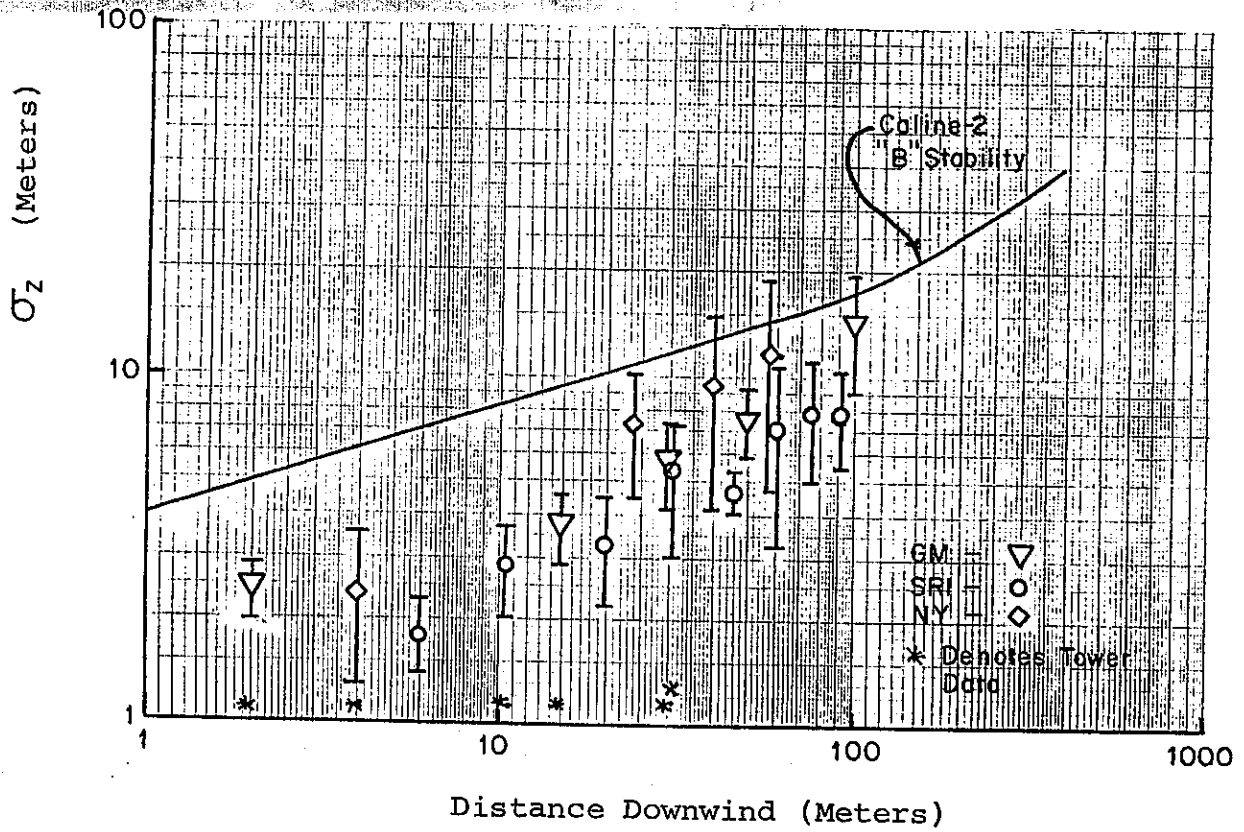


Fig. 9 σ_z as Calculated from Observed Concentrations Under "B" Stability ($U \geq 1.0 \text{ M/S}$, $\phi \geq 20^\circ$)

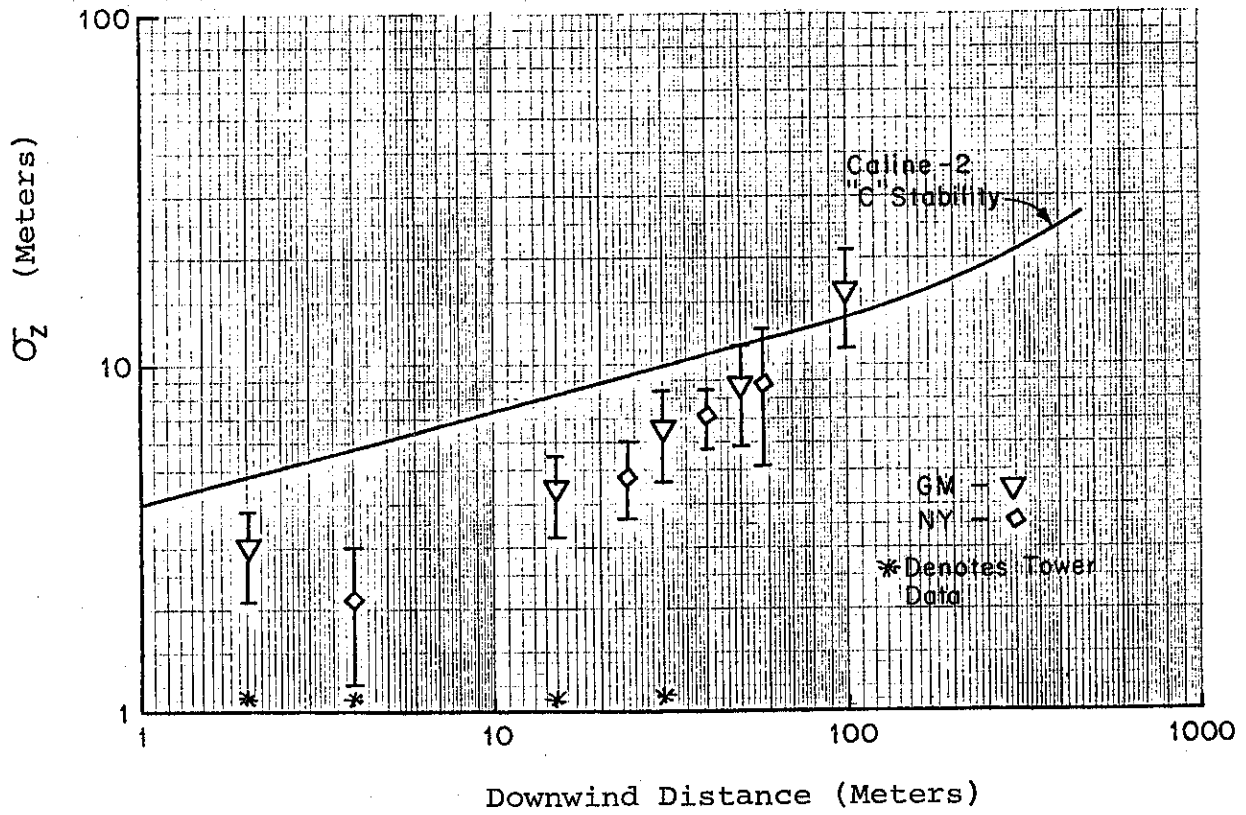


Fig. 10 σ_z as Calculated from Observed Concentrations Under "C" Stability ($U \geq 1.0$ M/S, $\phi \geq 20^\circ$)

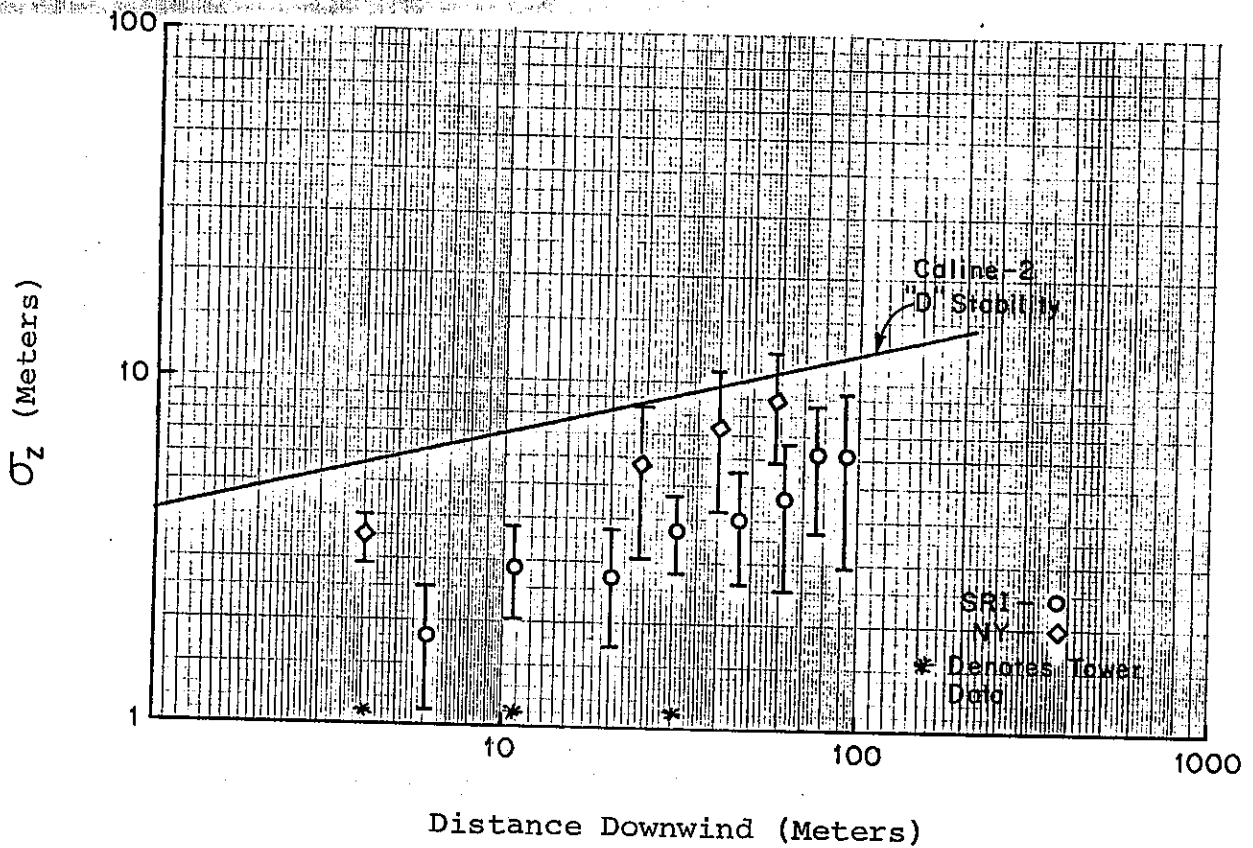


Fig. 11 σ_z as Calculated from Observed Concentrations Under "D" Stability ($U \geq 1.0 \text{ M/S}$, $\phi \geq 20^\circ$)

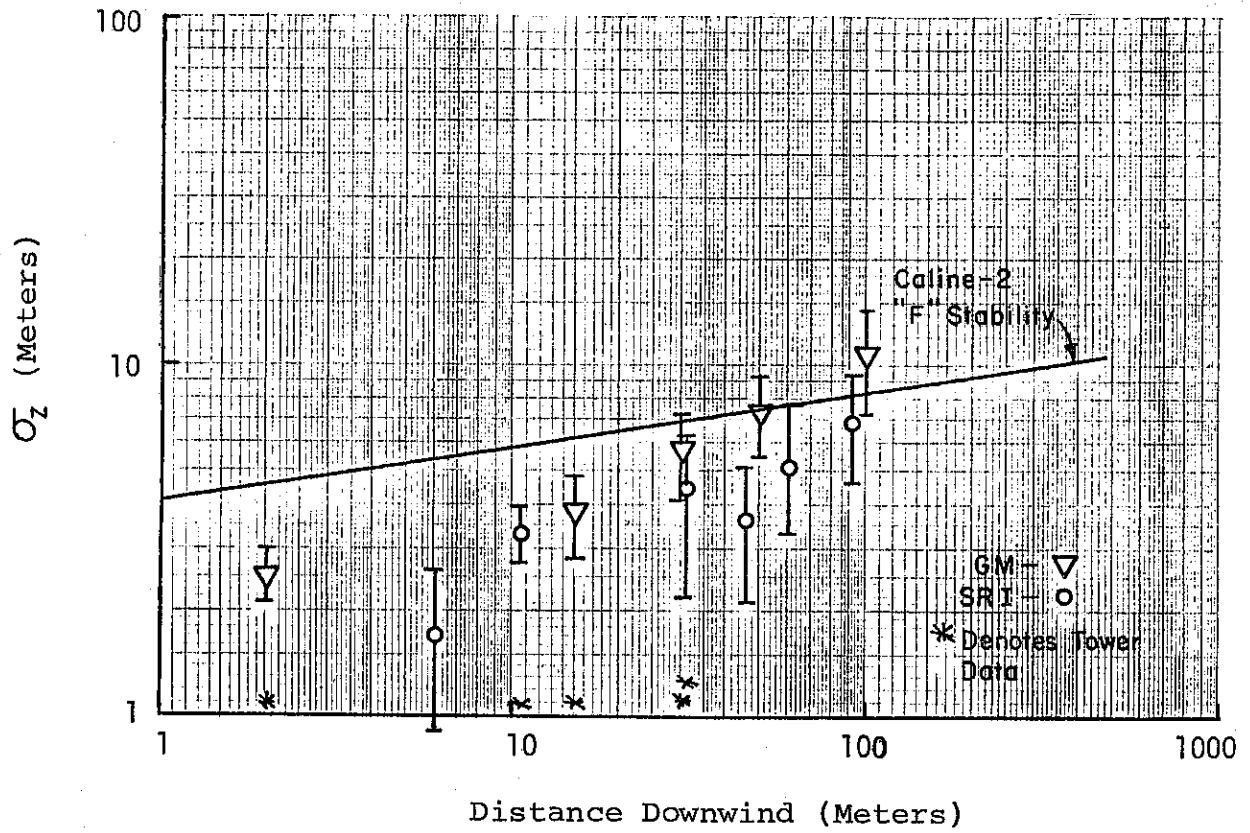


Fig. 12 σ_z as Calculated from Observed Concentrations Under "F" Stability ($U \geq 1.0 \text{ M/S}$, $\phi \geq 20^\circ$)

four stability classes studied. Also, the index of determination (r^2) is given to provide a relative measure of the scatter of the data and the correlation between σ_z and x ($r^2=1$ for perfect correlation).

Table 15

<u>Stability Class</u>	<u>Cases</u>	<u>r^2</u>	<u>α</u>	<u>β</u>
B	39	0.71	1.24	0.42
C	25 (GM only)	0.76	2.01	0.40
D	20	0.36	1.25	0.36
F	19 (GM only)	0.87	2.00	0.32

A power function such as $\sigma_z = \alpha x^\beta$ may be equivalently stated as:

$$\ln \sigma_z = \ln \alpha + \beta \ln x$$

where α can be thought of as the initial σ_z at the downwind edge of the freeway ($\sigma_z = \alpha$ when $x = 1$ meter), and β represents the rate of change of $\ln \sigma_z$ with $\ln x$, or slope. The results in Table 15 show a clear organization of β with respect to stability class. For more unstable conditions σ_z is increasing more rapidly with downwind distance, as would be expected. No such organization emerges for α , however.

Because of the suspected dominance of traffic-induced turbulence near the freeway, it was felt that α should be predicted by parameters that characterize the traffic flow rather than atmospheric stability. The likely candidates were traffic volume, vehicle speed, or some combination of the two. The GM data could not be used for this analysis since traffic volume and speed were held constant during their studies. The NY data base

came from a preliminary report for which no traffic data were available. Also, high residuals had already made their use questionable. The SRI data base did contain traffic volumes and speed measurements, however, and was used to determine the effects of these variables on σ_z estimates made at the 10.7 m tower.

A series of simultaneous temporal plots of σ_z , traffic volume (VPH), traffic speed (SPD), and wind speed (U) was made to see if any clear correlation existed (see Figures 13 thru 15). Naturally, an inverse relation between VPH and SPD was observed. But further examination of the plots did not support the expected direct relation between σ_z and either VPH or SPD. Instead, the values of σ_z at the closer tower seemed to be inversely related to the wind speed.

The two primary modes of turbulent mixing, bouyant and mechanical, are considered to be significantly augmented by the traffic flow. Additional bouyant turbulent kinetic energy is supplied from the waste heat emissions of the vehicles(10). Also, mechanical turbulent kinetic energy is added in the form of turbulent wakes accompanying vehicle motion(9). For purposes of the new model development, however, bulk indicators of the bouyant and mechanical components of turbulence due to the traffic were used. VPH was taken to represent the waste heat loading, hence the energy available to form bouyant turbulence. The term $VPH \cdot SPD^2$, as a measure of the total kinetic energy of motion of the traffic stream, was taken to represent the mechanical turbulence generated by the traffic flow.

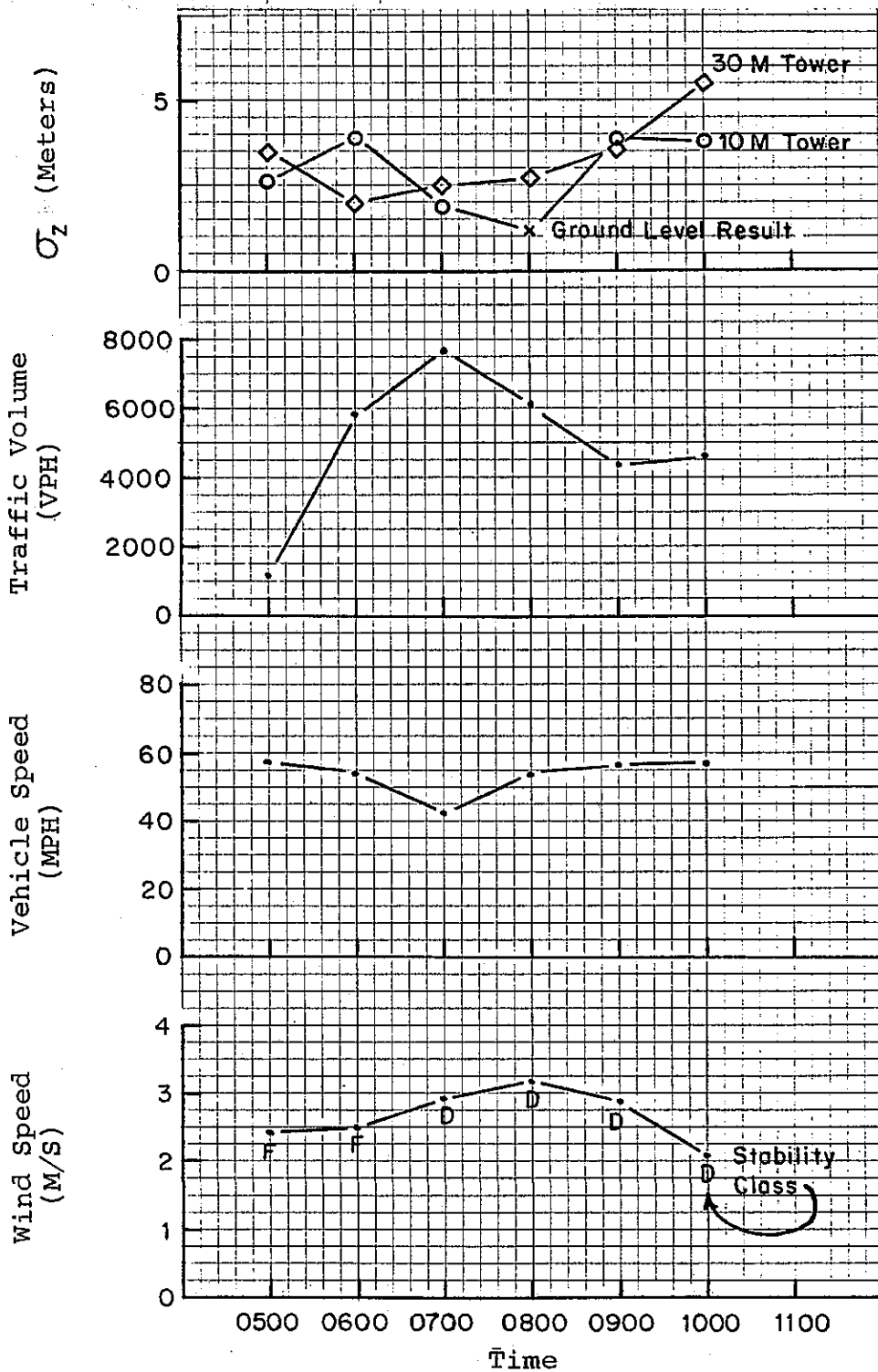


Fig. 13 Temporal Patterns for January 28, 1975 (SRI At-Grade Site)

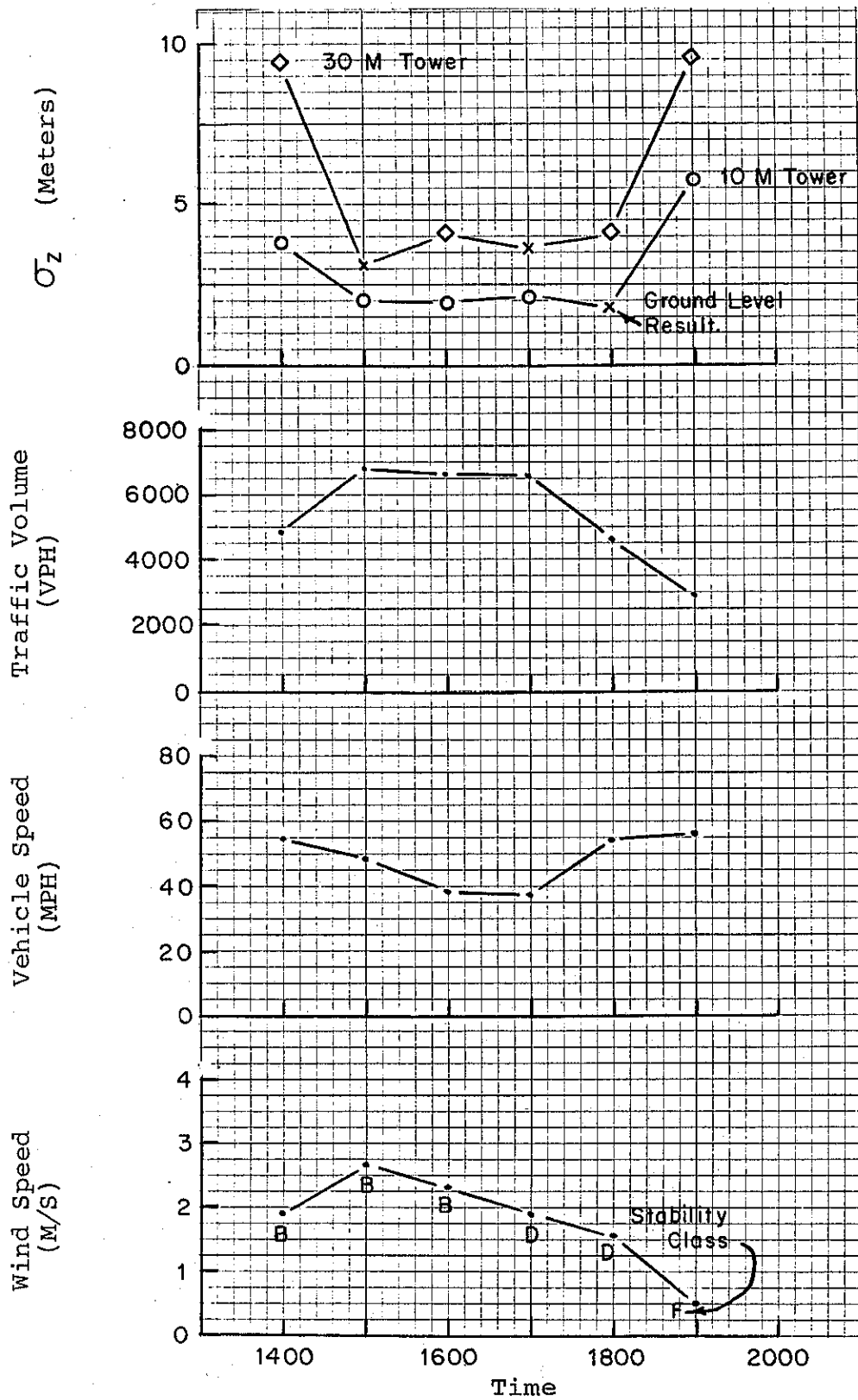


Fig. 14 Temporal Patterns for January 30, 1975 (SRI At-Grade Site)

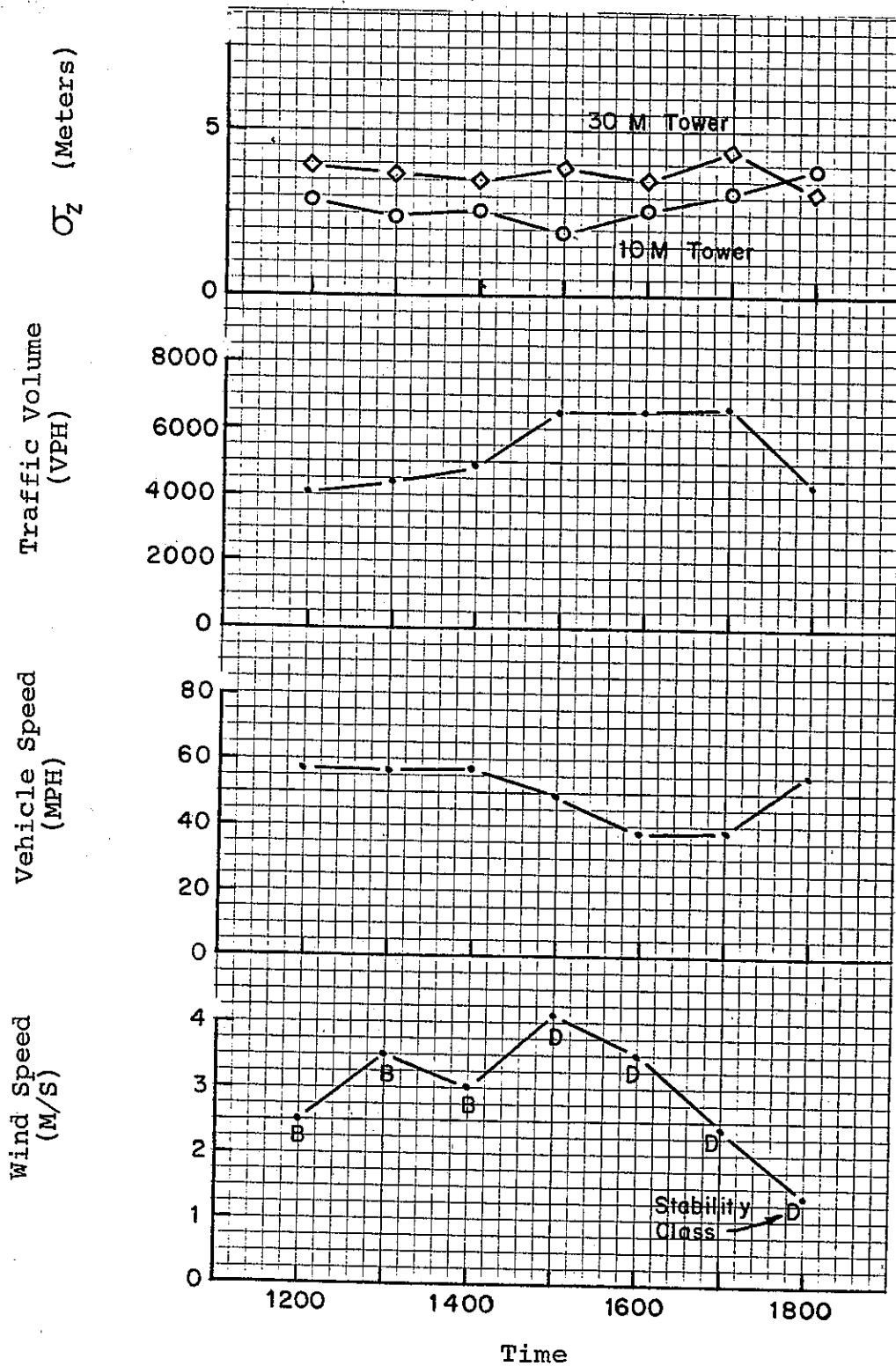


Fig. 15 Temporal Patterns for February 5, 1975 (SRI At-Grade Site)

Both VPH and $VPH \cdot SPD^2$ were plotted against σ_z measured at the 10.7 meter tower for $U \geq 1.0$ m/s (see Figures 16 and 17). Absolutely no correlation was exhibited.

Next, measures of roadway turbulence derived from SRI bivane data at $z = 2.0$ meters were compared to VPH and $VPH \cdot SPD^2$ (Figures 18 and 19). In these plots, σ_{ϕ_r} and σ_{θ_r} were computed as follows:

$$\sigma_{\phi_r} = \left(\sigma^2_{\phi_{\text{median}}} - \sigma^2_{\phi_{30M \text{ upwind}}} \right)^{\frac{1}{2}} = \text{Standard deviation of the vertical wind angle due to roadway turbulence}$$

$$\sigma_{\theta_r} = \left(\sigma^2_{\theta_{\text{median}}} - \sigma^2_{\theta_{30M \text{ upwind}}} \right)^{\frac{1}{2}} = \text{Standard deviation of the horizontal wind angle due to roadway turbulence}$$

The graphs show that for most normal freeway traffic flows, the roadway turbulence terms remain within a relatively constant band and that the magnitude of this turbulence is significant. Only for the one low flow condition, do σ_{ϕ_r} and σ_{θ_r} drop below these bands. Figure 20 shows a similar plot for σ_w (standard deviation of the vertical wind speed) data at $z = 3.8$ meters against $VPH \cdot SPD^2$. The interpretation is the same at this higher level.

The currently accepted method for estimating σ_y from bivane data is, $\sigma_y = \sigma_{\theta} X \cdot f(X)$ which derives from $\sigma_y = \sigma_v t \cdot f\left(\frac{t}{\tau_L}\right)$, where τ_L = Lagrangian Time Scale (5).

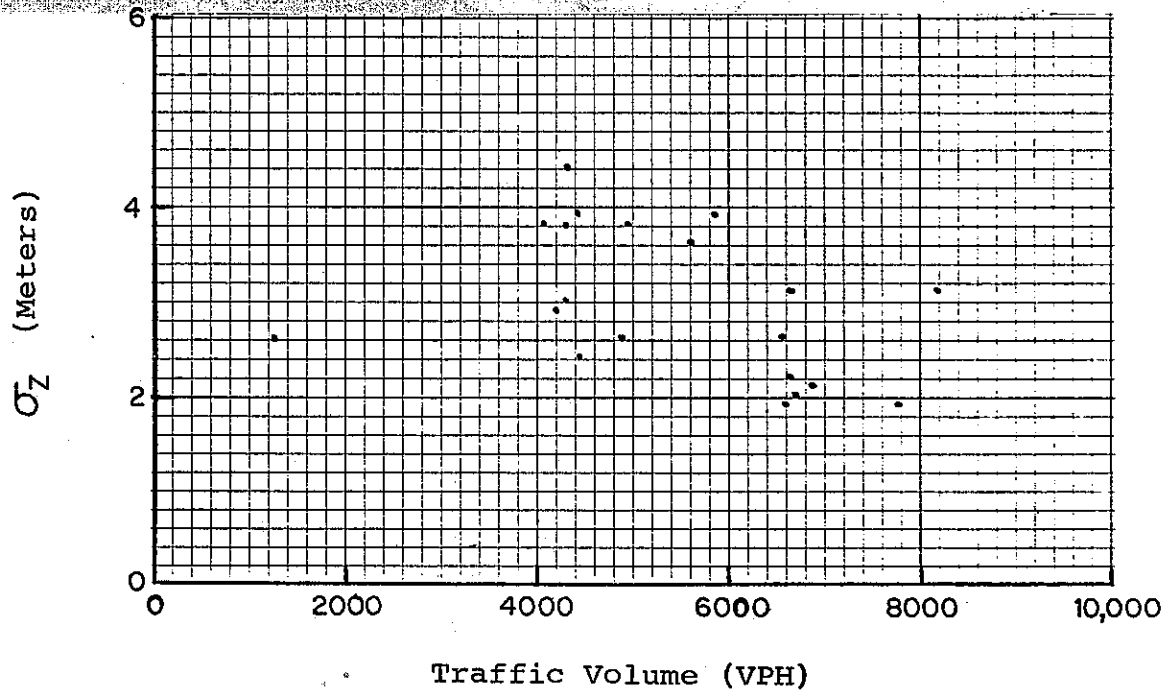


Fig. 16 Best Fit σ_z @ 10 Meter Tower
Versus Traffic Volume
(SRI At-Grade Site, $U > 1\text{M/S}$)

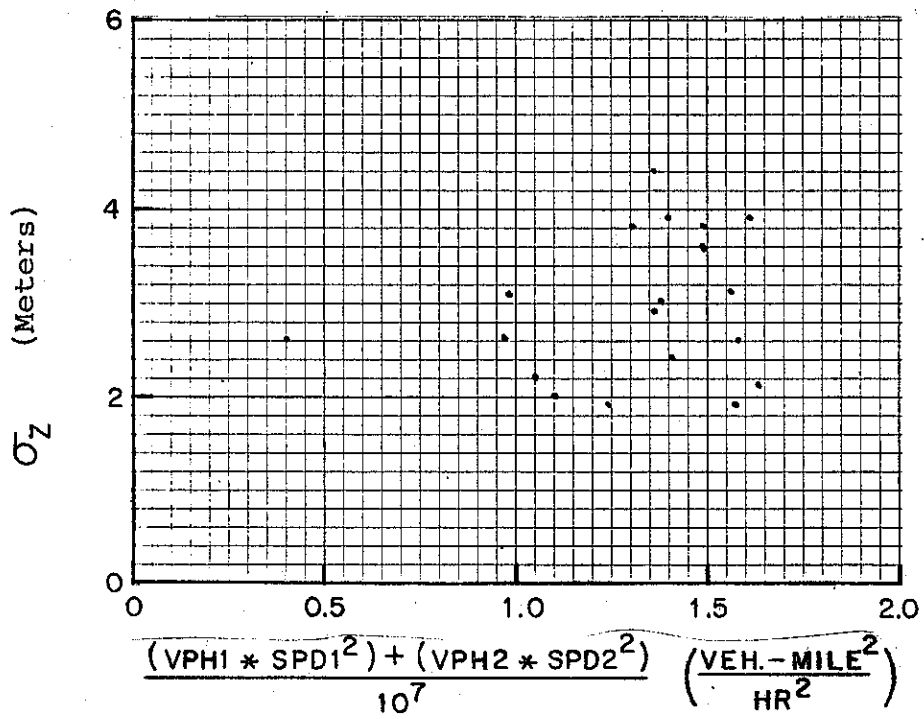
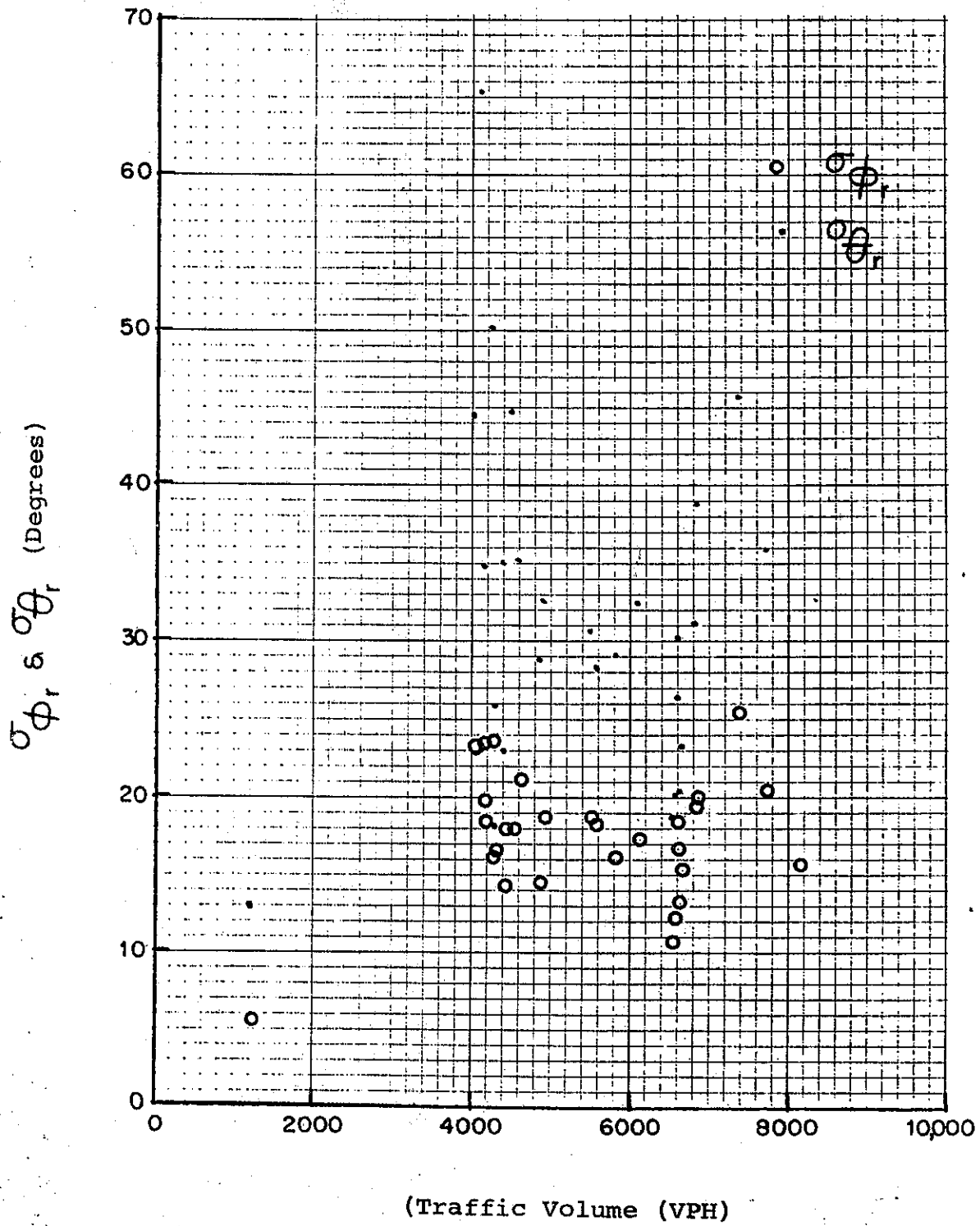


Fig. 17 Best Fit σ_z @ 10 Meter Tower
Versus Traffic Energy Index
(SRI At-Grade Site, $U \geq 1 M/S$)



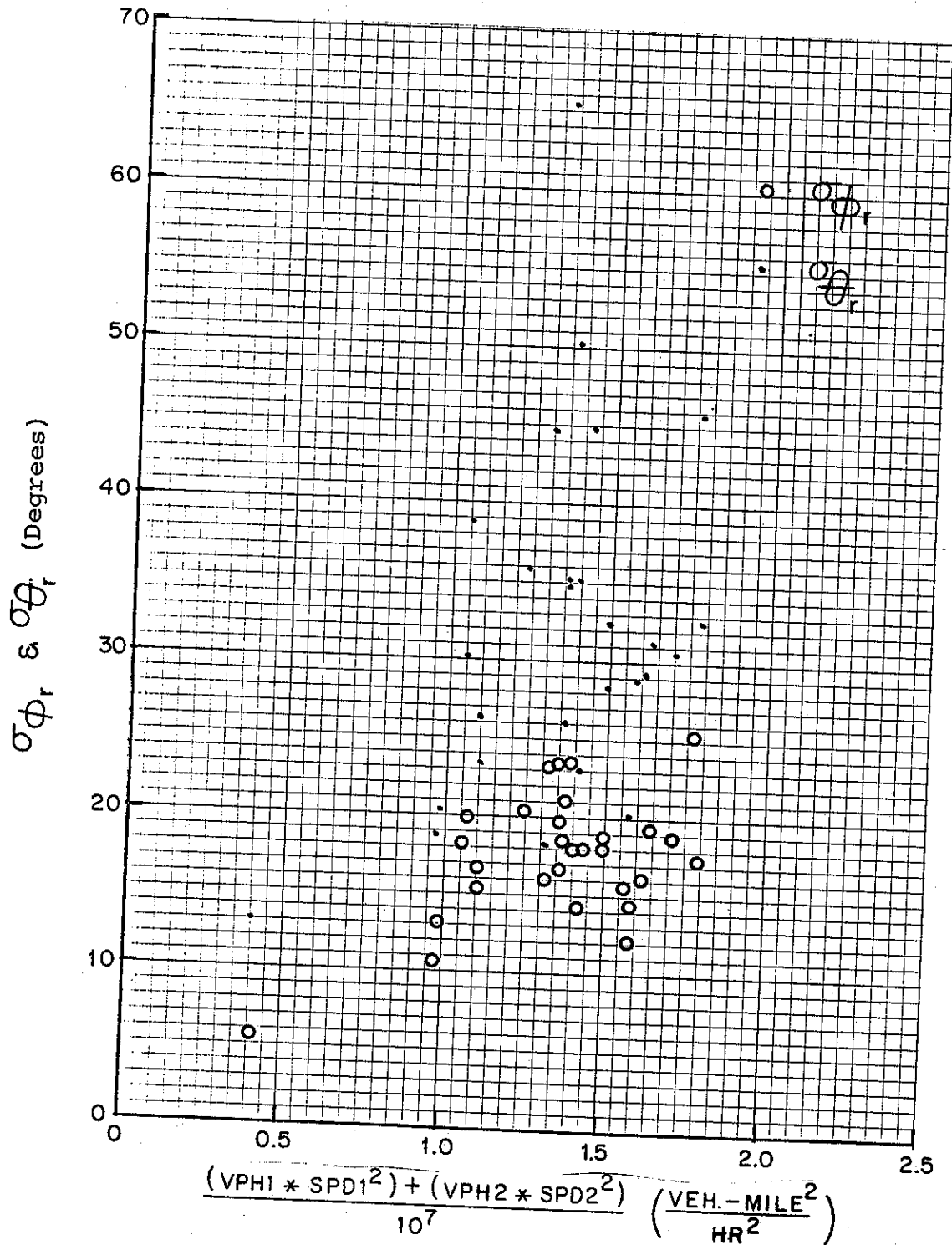


Fig. 19 Roadway Turbulence (σ_{ϕ_r} & σ_{θ_r}) Measured @ 2 Meter Height, versus Traffic Energy Index - SRI Data

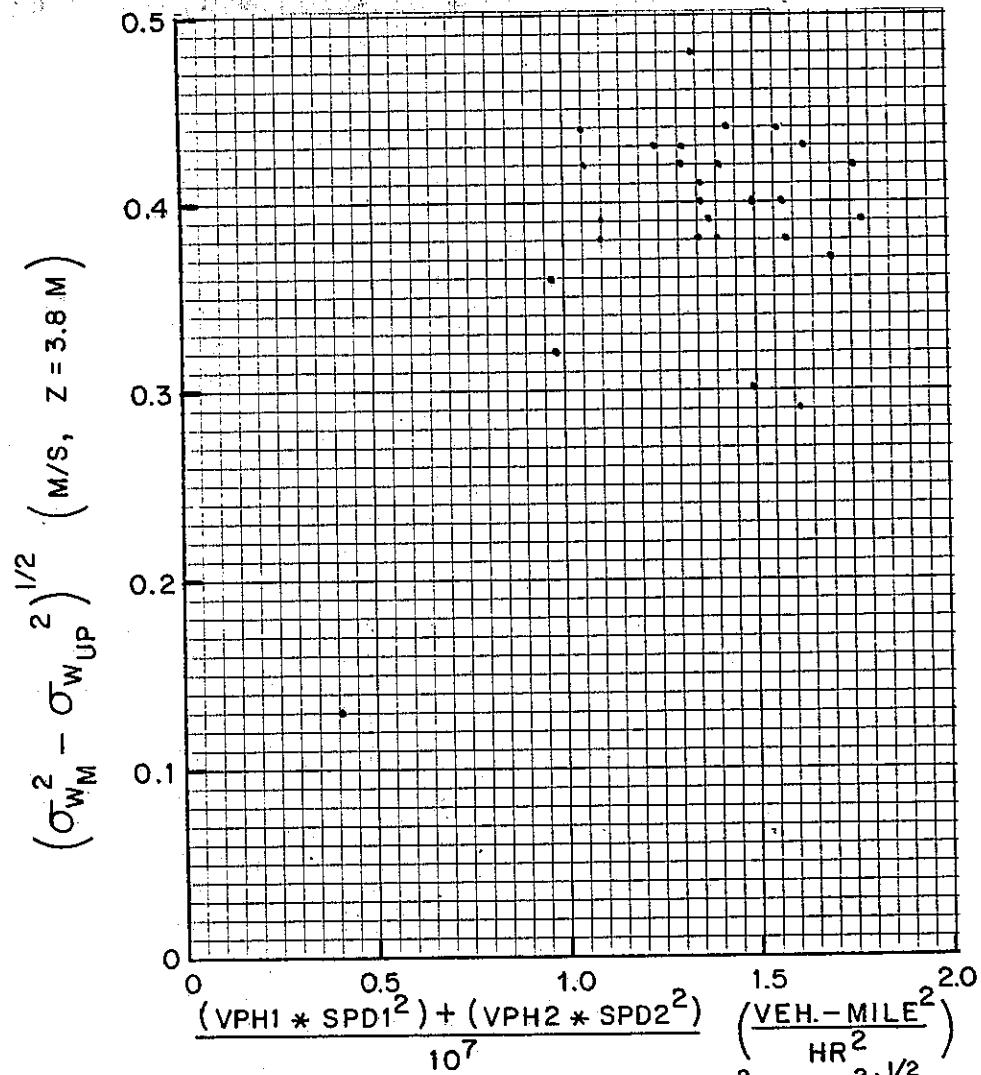


Fig. 20 Roadway Turbulence, $(\sigma_{WM}^2 - \sigma_{WUP}^2)^{1/2}$,
 Measured at Z = 3.8 Meters versus
 Traffic Energy Index - SRI Data

The SRI UVW anemometer results were compared to the σ_z estimates at the 10.7 meter tower to evaluate the following analogous functions for σ_z :

$$\sigma_z = \sigma_\phi \chi \cdot g(\chi)$$

$$\sigma_z = \sigma_w t \cdot g\left(\frac{t}{\tau_L}\right)$$

Values of $\sigma_\phi \chi$ and $\sigma_w t$ were computed as follows:

$$\sigma_\phi \chi = 18.3 \sigma_{\phi \text{ median}} + 10.7 \sigma_{\phi \text{ 10M. downwind}}$$

$$\sigma_w t = \left(\frac{18.3}{U}\right) \sigma_{w \text{ median}} + \left(\frac{10.7}{U}\right) \sigma_{w \text{ 10M. downwind}}$$

The results, shown in Figure 21, are far from conclusive but do give a reasonable value of 0.5 for $g(t/\tau_L)$ at 10 meters downwind from the freeway

The graph also points out the importance of considering the travel time, hence wind speed, when predicting σ_z near a freeway.

To help explain the foregoing results and provide a practical method for predicting α (initial σ_z) the following hypothesis is proposed. Assume that the dominant source of turbulent mixing near the highway is mechanical in nature and thus related to $VPH \cdot SPD^2$. Because of the inverse relation between VPH and SPD, the magnitude of $VPH \cdot SPD^2$ on an urban freeway remains relatively constant during the day from say 0600 to 2000 hours. Thus, during this time period the amount of initial mixing at the freeway is predominantly determined by the residence time within the "mixing cell". If this were true, one would expect an inverse relationship between the initial σ_z and U.

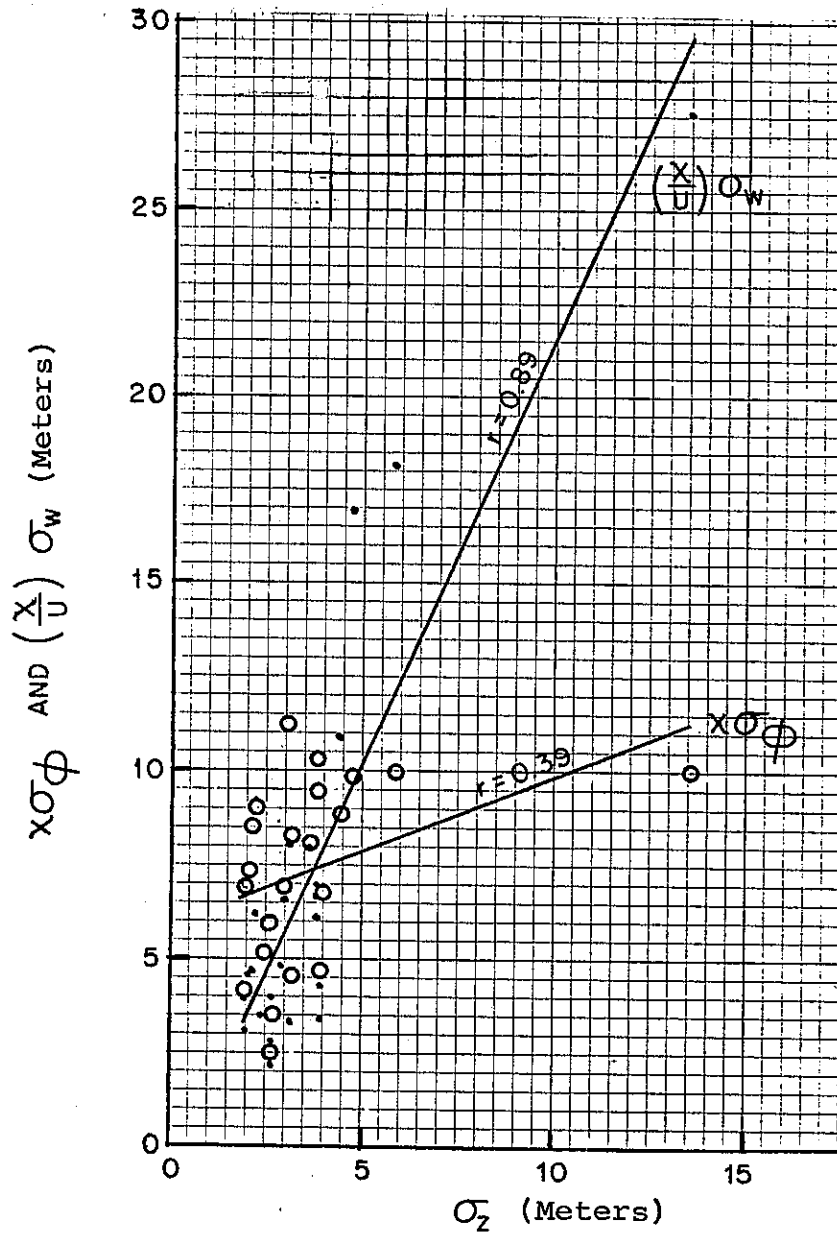


Fig. 21 Evaluation of $g(x)$ and $g(t/T_L)$ Functions
 SRI Data, Bivane Results
 at $Z = 3.8$ Meters

To test this hypothesis, data from the GM, SRI and LA field studies were used. Estimates of σ_z for the LA study were based on ground level measurements at the edge of the San Diego Freeway (Site 3) for the $75^\circ \leq \phi \leq 81^\circ$, with no tracer control. These results were included because they offered a wider range of wind speeds than the tracer studies. The results are shown in Figure 22. The wind speeds were measured upwind of the freeway at distances from 30 to 40 meters and heights ranging from 3.8 meters for the SRI data to 8.8 meters above the road surface for the LA data. The GM and LA results agree quite closely. The SRI results are somewhat higher, but this would be expected since these σ_z 's were computed 10.7 meters downwind from the freeway, while the GM and LA results were 1 to 2 meters downwind.

The implications of Figure 22 seem clear, but another possible hypothesis could explain the exhibited behavior. If the traffic flow so affected the mean wind speed such that the wind speed immediately downwind of the freeway remained constant and independent of the upwind wind speed, the same type of plot would be expected. Paired upwind and downwind wind speeds for the SRI data at $z = 3.8$ meters shown in Figure 23 demonstrate that this is not the case. A similar check of the GM wind results revealed the same approximate 1 to 1 relationship.

The GM and LA results were combined (70 cases, $r^2 = 0.90$) to compute the final version of the initial σ_z equation. This yields an overall model for σ_z values (in meters) of the form, $\sigma_z = \alpha x^\beta$, for a range of 100 meters downwind of a freeway (see Table 16).

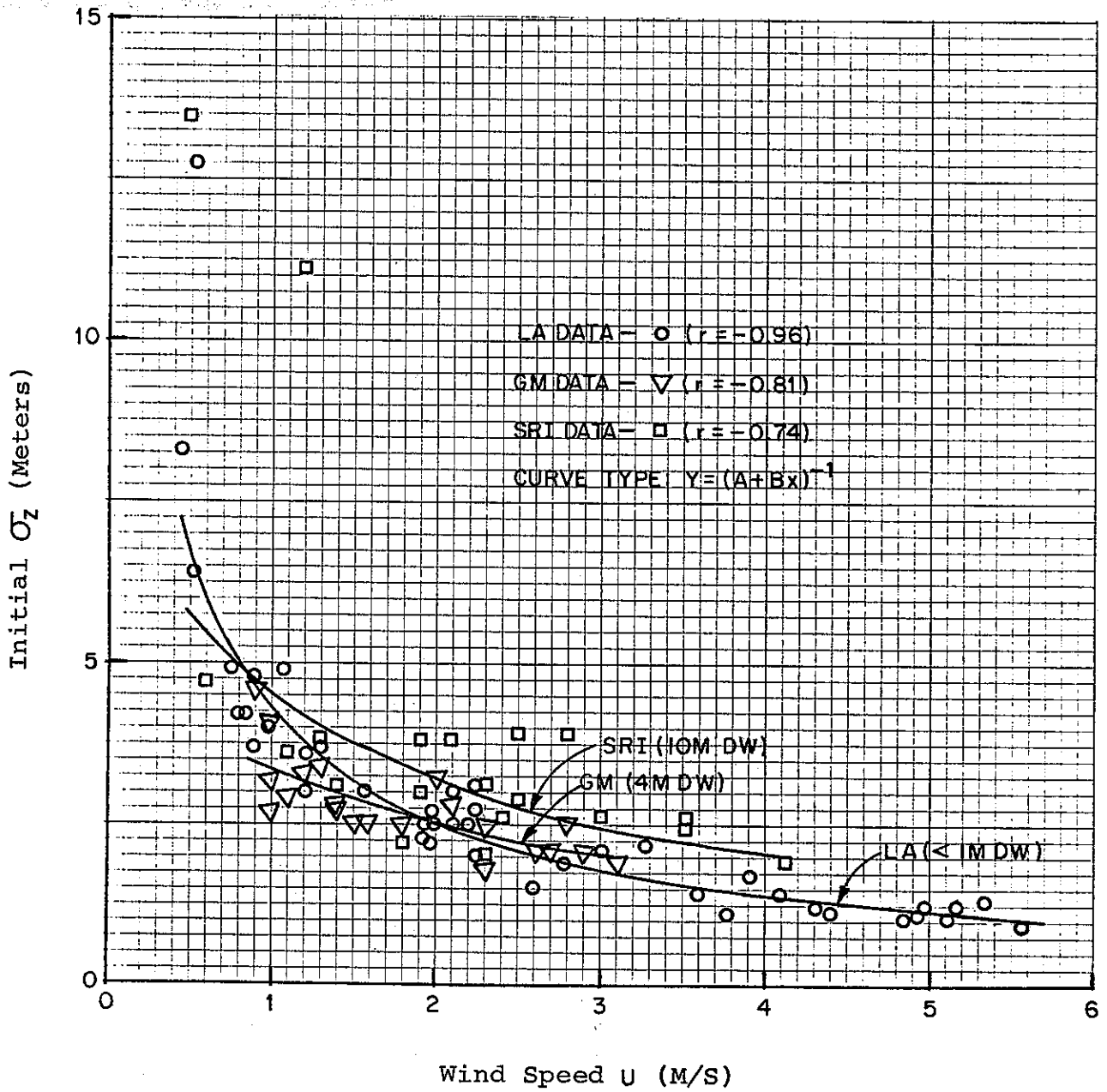


Fig. 22 Best Fit σ_z Near Downwind Edge of Roadway Versus Wind Speed ($\phi \geq 45^\circ$)

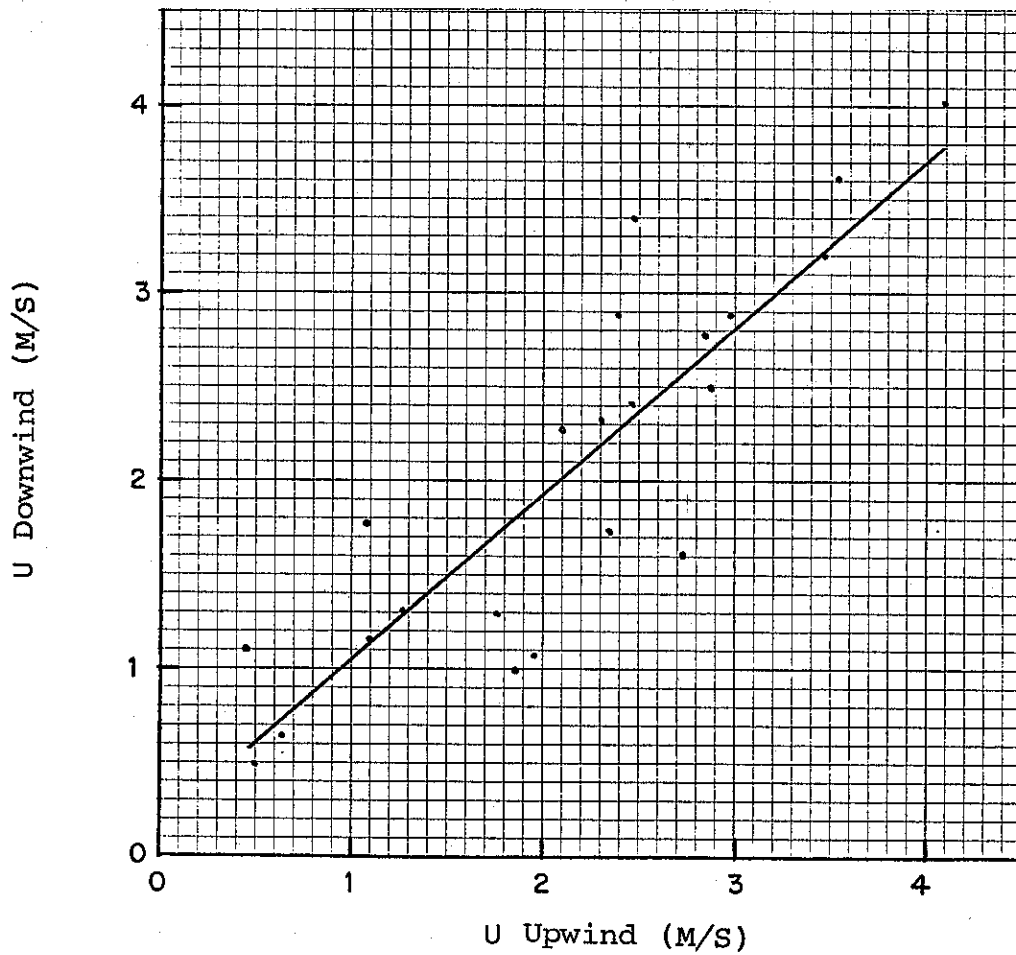


Fig. 23 Paired Upwind and Downwind Values of U at Z = 3.8 Meters SRI Data

Table 16

<u>Stability Class</u>	<u>α (Initial σ_z)</u>	<u>β</u>
B	$(0.081 + 0.16U)^{-1}*$	0.42
C	" "	0.40
D	" "	0.36
F	" "	0.32

*U measured upwind at $z = 4$ to 8 meters in m/s.

A comparison of σ_z curves between those proposed in this report and the current CALINE2 curves is shown in Figure 24. The tendency for CALINE2 to underpredict CO concentrations near the freeway for neutral to unstable crosswind conditions is evident if one accepts the new curves as accurate. The plot also shows the extreme importance of correctly predicting the initial σ_z .

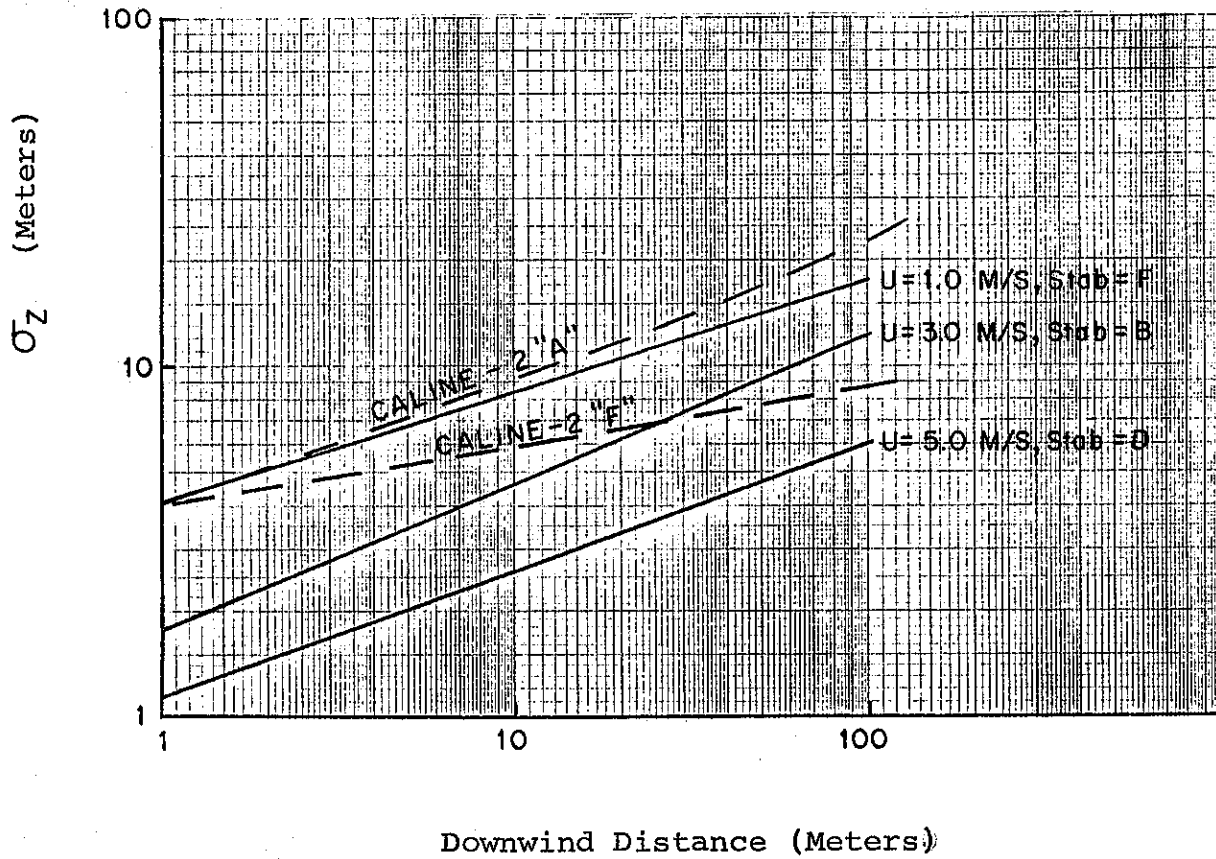


Fig. 24 Comparison of Present CALINE-2 Curves to Three Representative Cases of Recommended Sigma Z Curve Model

REFERENCES

1. Noll, K. E., Miller, T. L. and Claggett, M. (1978): A Comparison of Three Highway Line Source Dispersion Models, Atmospheric Environment, v. 12, pp 1323-1329.
2. Maldonado, C. and Bullin, J. A. (1977): Modeling Carbon Monoxide Dispersion from Roadways, Environmental Science and Technology, v. 11, No. 12, pp 1071-1076.
3. Benson, P. E. (1978): Validation of the Line Source Air Pollutant Model, CALINE-2, Unpublished Termination Report.
4. California Division of Highways (1970): Project Smoke, Unpublished Study.
5. Hanna, S. R., Briggs, G. A., Deardorff, J., Egan, B. A., Gifford, F. A. and Pasquill, F. (1977): AMS Workshop on Stability Classification Schemes and Sigma Curves - Summary of Recommendations, Bulletin American Meteorology Society, v. 58, No. 12, pp 1305-1309.
6. Johnson, W. B. (1974): Field Study of Near Roadway Diffusion Using a Fluorescent Dye Tracer, Symposium on Atmospheric Diffusion and Air Pollution. American Meteorological Society, Santa Barbara, California, September 9 - 13, 1974, pp 261-266.
7. Draxler, R. R. (1976): Determination of Atmospheric Diffusion Parameters, Atmospheric Environment, v. 10, pp 99-105.

8. Pasquill, F. (1976): Atmospheric Dispersion Parameters in Gaussian Plume Modeling, part II, U. S. Environmental Protection Agency, Research Triangle Park, North Carolina, June 1976.
9. Rao, S. T. and Sedefian L. (1978): Characteristics of Turbulence and Dispersion of Pollutants Near Major Highways, New York State Department of Environmental Conservation, Unpublished Study.
10. Dabberdt, W. F. (1976): Experimental Studies of Near Roadway Dispersion, Proceedings 69th APCA Annual Meeting, Portland, Oregon.
11. Chock, D. P. (1977): General Motors Sulfate Dispersion Experiment - An Overview of the Wind, Temperature and Concentration Fields, Atmospheric Environment, v. 11, pp. 553-559.
12. Cadle, S. H., Chock, D. P., Heuss, J. M. and Monson, P. R. (1976): Results of the General Motors Sulfate Dispersion Experiment, GMR-2107, General Motors Corporation, Warren, Michigan, March 18, 1976.
13. Dabberdt, W. F. (1975-78): Studies of Air Quality On and Near Highways, Project 2761, Stanford Research Institute, Menlo Park, California.
14. Rao, S. T. and others (1978): Dispersion of Pollutants Near Highways, Preliminary Tracer Results (unpublished), New York State Department of Environmental Conservation, Albany, N.Y.

15. Bemis, G. R. and others (1977): Air Pollution and Roadway Location, Design and Operation - Project Overview, California Department of Transportation, Sacramento, California, September, 1977.
16. Draper, N. R. and Smith H. (1966): Applied Regression Analysis, John Wiley and Sons, Inc., New York.
17. SethuRaman, S. and Tichler, J. (1977): Statistical Hypothesis Tests of Some Micrometeorological Observations, Journal of Applied Meteorology, v. 16, No. 5, pp. 455-461.
18. Deardorff, J. W. and Willis, G. E. (1975): A Parameterization of Diffusion into the Mixed Layer, Journal of Applied Meteorology, v. 14, pp. 1415-1458.
19. Lovelock, J. E. (1971): Nature, v. 231, p. 279.
20. Dietz, R. N. and Cote, E. A. (1973): Tracing Atmospheric Pollutants by Gas Chromatographic Determination of Sulfur Hexafluoride, Environmental Science and Technology, v. 7, No. 4, pp. 338-342.
21. Claffey, P. J. (1974): Motor Vehicle Energy Consumption: A Function of Diverse Factors, Caltech Seminar, June, 1974.
22. Apostolos, J. A., Shoemaker, W. R. and Shirley, E. C. (1978): Energy Factor Handbook - Appendix A, California Department of Transportation.
23. Bettes, W. H. (1974): On the Design of Automobiles for Lower Air Resistance, Caltech Seminar, June, 1974.